Contrib Mineral Petrol (1998) 133: 217–234

Simon Turner · Frank McDermott · Chris Hawkesworth · Pavel Kepezhinskas

A U-series study of lavas from Kamchatka and the Aleutians: constraints on source composition and melting processes

Received: 24 September 1997 / Accepted: 7 July 1998

Abstract New data are presented for lavas from the Kamchatka Peninsula and the Aleutian arc. Radiogenic isotopes are strikingly homogeneous in the Kamchatka lavas and although incompatible trace element ratios exhibit much greater variability, much of this appears to result from shallow level, crystal fractionation. The data reveal little systematic across-arc change in radiogenic isotopes or trace element ratios. The Nd and Pb isotope data overlap those for Pacific MORB and limit the amount of sediment that could be incorporated in the mantle source region to $<1\%$ which is insufficient to account for the observed La/Ta ratios (50–68) in the high-MgO lavas. The lack of a positive correlation between La/Ta and depth to the slab suggests that melt–wall rock interaction was not important in controlling this ratio. Instead it is inferred that La/Ta increased during partial melting and that $D_{La}/D_{Ta} = 0.11$–0.06, possibly due to residual amphibole. Ba, U, Sr and Pb were added to the source by an aqueous fluid from the subducting slab and its inferred isotopic composition indicates that this fluid was derived from the altered oceanic crust. The addition of U resulted in a large range of $(^{238}U/^{232}Th)$ from 0.79–2.48 similar to that observed in the Mariana and Lesser Antilles island arcs. However, $(^{230}Th/^{232}Th) = 0.79$–$2.34$, and the majority of samples lie close to the equiline indicating that the time since U/Th fractionation is generally ≥150 thousand years. The large width of the volcanic zone is assumed to reflect protracted fluid release from the subducting slab over the depth interval 170–380 km possibly coupled with extension across the Central Kamchatka Depression. The data from the Aleutians contrast strongly with those from Kamchatka. Radiogenic isotope data indicate that the Aleutian lavas contain a significant recycled sedimentary component, consistent with elevated $^{10}Be/^{9}Be$ ratios. The Aleutian lavas have $(^{230}Th/^{232}Th) = 0.79$–$2.34$ and exhibit a significant range of U/Th disequilibria $[(^{238}U/^{230}Th) = 0.75$–$1.01]$. However, $^{10}Be/^{9}Be$ is positively correlated with $(^{238}U/^{230}Th)$ suggesting that the ^{10}Be signal was carried by the aqueous fluid from the slab. The U/Th disequilibria for the Aleutian lavas lie close to a 30 thousand year reference line suggesting that this fluid was released from the slab ~30 thousand years ago similar to recent estimates from the Lesser Antilles, Marianas, and Tonga-Kermadec island arcs from which it is inferred that fluid addition was the trigger for partial melting. Given that the rate of convergence in Kamchatka is similar to that in the Aleutians, Marianas and Tonga-Kermadec the inferred greater time since fluid release in Kamchatka requires further investigation.

S. Turner (✉) · C. Hawkesworth
Department of Earth Sciences, The Open University, Milton Keynes, MK7 6AA England

F. McDermott
Department of Geology, University College Dublin, Belfield, Dublin 4, Ireland

P. Kepezhinskas
Department of Geology, University of South Florida, Tampa, FL 33620-5200, USA

Editorial responsibility: W. Schreyer

Introduction

Destructive plate margins are major sites for material exchange between the mantle and crust yet there remains considerable uncertainty over the specific sources and rates of transfer of individual elements (see Hawkesworth et al. 1993 and Pearce and Peate 1995 for recent reviews). On the basis of incompatible trace element and Sr, Nd and Pb isotope ratios, a number of studies have identified separate contributions from subducted sediments, a slab dehydration-derived fluid and the mantle wedge (e.g. Kay 1980; Ellam and Hawkesworth 1988; McDermott et al. 1993; Miller et al. 1994; Turner et al. 1996, 1997; Elliott et al. 1997; Hawkesworth et al. 1997a,

b). In light of such models, Kamchatka may be an important end-member of island arc systems because Kersting and Arculus (1995) have argued that there is little or no sediment contribution to the lavas in this arc.

The U-series isotopes, in principle, have the potential to constrain the rates of transfer of various components in arc lavas. The ^{238}U-^{230}Th isotope disequilibria record U/Th fractionation on time scales of < 350 ka and because U is highly mobile in oxidising aqueous fluids and Th is not (Bailey and Ragnarsdottir 1994; Brenan et al. 1995; Keppler 1996), the observation of ^{238}U excesses in many island arc lavas has been ascribed to the role of a slab-derived fluid component (e.g. Gill and Williams 1990; McDermott and Hawkesworth 1991; Condomines and Sigmarsson 1993; Hawkesworth et al. 1997b). More recent studies have looked in detail at the U-Th systematics within individual arcs (Gill et al. 1993; Reagan et al. 1994; Turner et al. 1996, 1997; Elliott et al. 1997) and these suggest that the timescale between U/Th fractionation caused by fluid addition to the wedge and eruption may typically be 30–50 ka (Turner et al. 1996, 1997; Elliott et al. 1997; Turner and Hawkesworth 1997).

Most of the U-series isotope studies to date have looked at along-arc variations in order to elucidate the relative contributions of the different source components. Much less is known about across-arc variations. If melting and fluid addition take place at the slab-mantle wedge interface (e.g. Tatsumi et al. 1986), then how is the increasing depth of partial melting reflected in the compositions of the lavas produced? For example, does the role of fluids diminish across arc due to declining amounts of fluids being released from the slab? Alternatively, if fluids migrate broadly horizontally through the wedge from the point of dehydration on the slab (Davies and Stevenson 1992), then how far can such fluids penetrate across the wedge and what constraints does this place on the thermal structure of the wedge? In the only previous U-series study to have looked at across-arc variations, Gill et al. (1993) found little variation between the volcanic front in the East Bismark arc and lavas from volcanoes up to 240 km above the slab, and noted that the subduction signature only disappeared when the slab was at depths of ~400 km. These are interesting results and it is important to see if similar relationships hold for other arcs. To this end we have chosen to undertake a U-series study of the Kamchatka arc which contains active volcanoes ranging across the arc from 100 to 340 km above the subducting slab where there is currently active intra-arc extension.

The Kamchatka arc

Kamchatka lies at the junction of two island arc systems in the north Pacific formed by subduction of Mesozoic Pacific oceanic crust beneath the Eurasian plate to the west (Kurile–Kamchatka arc) and the North American plate to the north (Aleutian arc). The junction with the Aleutian arc divides the Kamchatka peninsula into northern and central segments and the Petropavlovsk fault zone separates the southern and central segments (Fig. 1). The southern segment is comprised of Kurile-type volcanic basement whereas the central and northern segments are comprised of 30–40 km thick crust formed from accreted Mesozoic and Tertiary oceanic and island arc terrains (e.g. Geist et al. 1994). Intra-arc extension has resulted in a large graben oriented parallel to the trench ~200 km above the Benioff zone known as the Central Kamchatka Depression (CKD) which separates the Eastern Volcanic Front (EVF) from the rear arc volcanic zone of the Sredinny Ridge which is now largely inactive except for one volcano, Ichinsky (see Fig. 1). The northern segment was formed by westwards subduction of newly formed oceanic crust produced by short-lived spreading in the Komandorsky Basin (Baranov et al. 1991). However, the volcanism here apparently ceased around 2 Ma (Kepezhinskas et al. 1995,

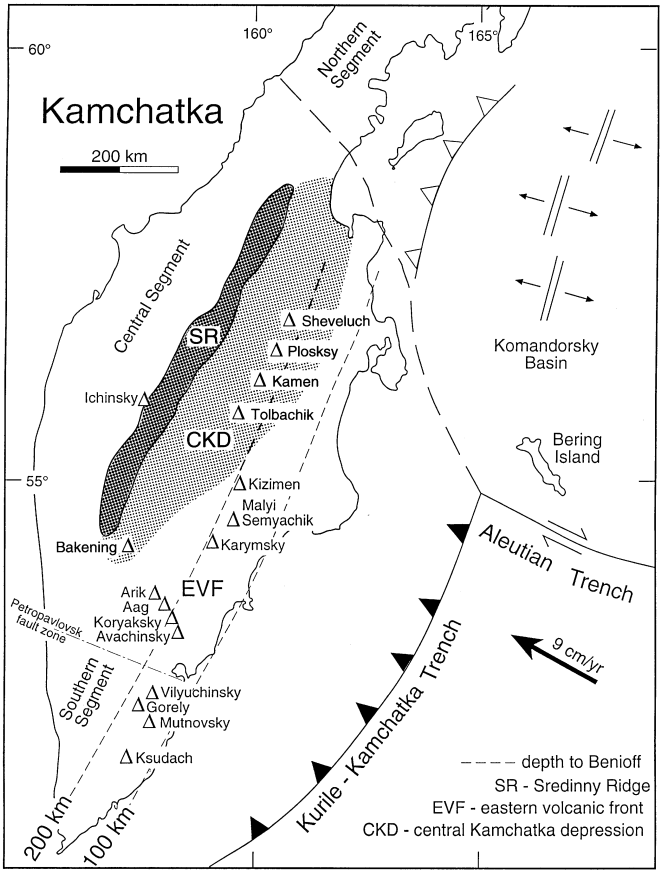

Fig. 1 Map of Kamchatka showing the regional tectonic structure, the locations of the volcanoes from which samples have been analysed and contours of the depth to Benioff zone. Lavas from volcanoes in the Eastern Volcanic Front have been subdivided into those (Arik to Kizimen) in the north (*Nth. EVF*) which lie trenchwards of the Central Kamchatka Depression (*CKD*) intra-arc extensional zone and those (Aag to Ksudach) further south (*Sth. EVF*) which are unlikely to have been influenced by rear arc magma extraction in the CKD

1996) and is thus too old for a U-series study. In contrast, the CKD and EVF in the central and southern segments form one of the world's most active volcanic areas. Subduction occurs orthogonally to the arc at ~9 cm a^{-1} and the Benioff zone dips at 40–50° reaching depths of ~170–220 km beneath the EVF and ~200–260 km beneath the CKD (Fig. 1, Kepezhinskas et al. 1996, 1997 and references therein).

The sediments being carried on the north-western Pacific plate are predominantly composed of siliceous oozes with subordinate ash-rich, silty and clay horizons (Rea 1993) and these have been analysed by Kay and Kay (1988), McDermott and Hawkesworth (1991), Bailey (1993) and Kersting (1995). A lithologically weighted average composition of the ~364 m sediment pile intersected at ODP site 881 south of Kamchatka has been calculated by Plank and Langmuir (1998) based on analyses from the Kurile sediment package. However, a significant portion of the sediment entering the Kamchatka trench is being scraped off into a large accretionary wedge (Geist and Scholl 1994) and so both the amount of sediment being subducted, and the applicability of the lithologically weighted average composition are subject to some uncertainty in this arc.

Lavas from Kamchatka are largely tholeiitic to calc-alkaline and often highly magnesian. Some more K-rich lavas do occur, particularly in the northern segment along with adakites and Nb-rich lavas which contain abundant Na- and Nb-rich metasomatised mantle xenoliths (Kepezhinskas et al. 1995, 1996; Hochstaedter et al. 1996). These may reflect slab melts of the newly subducted, hot oceanic crust formed in the Komandorsky Basin (Kepezhinskas et al. 1997; Volynets et al. 1997) but due to their age are not considered further here. Of the active southern segment volcanoes, Hochstaedter et al. (1996) presented evidence that lavas from the CKD have slightly enriched Ce/Yb ratios whereas those from the EVF have slightly depleted Ce/Yb ratios and argued that this reflects depletion of the mantle wedge beneath the CKD as it convects from the rear towards the EVF. With respect to this, we have subdivided the EVF volcanoes into a northern group (Arik to Kizimen), which lies between the CKD and the trench, and those further south (Aag to Ksudach), which are beyond any influence of prior melt extraction beneath the CKD (Fig. 1). The Sr, Nd and Pb isotopes are generally very similar to Pacific MORB suggesting a relatively minor contributing role for the subducted sediments, though the northern segment lavas have slightly higher $^{143}Nd/^{144}Nd$ and lower $^{208}Pb/^{204}Pb$ ratios than lavas further south (Kepezhinskas et al. 1997). In a detailed study of Klyuchevskoy volcano in the northern CKD, Kersting and Arculus (1995) showed that addition of even a small amount of sediment would shift the Pb isotope ratios of the lavas from the Pacific MORB field to more radiogenic values. Accordingly, Kersting and Arculus (1995) suggested that Kamchatka represents an important end-member island arc where little or no sediment is involved in the arc magmas.

Analytical techniques

Twenty-five samples spanning the currently active CKD and EVF volcanoes as well as Ichinsky from the Sredinny Ridge were selected from the collection of Kepezhinskas et al. (1997) for analysis so as to encompass a range of distances from the trench and above the Benioff zone. Many of the lavas were taken from historic eruptions (see Table 1 for ages) and the great majority are less than 10,000 years old (detailed sample descriptions, locations and age constraints are given in Kepezhinskas et al. 1997). The lavas from Arik and Aag volcanoes (samples 26107 and 27077) are only poorly constrained to be Mid- to Late-Pleistocene and so the U-series results from these samples must be treated with caution as no age correction has been made to their ($^{230}Th/^{232}Th$) ratios. Additionally, seven samples from the Aleutian arc, including two xenoliths from Adak island, five of which were previously analysed for Be isotopes and B concentrations by Morris et al. (1990), were analysed for U-Th isotopes for comparison with the Kamchatka data.

Major and trace element and Sr, Nd and Pb isotope data for the CKD and EVF lavas, analysed here for U-Th isotopes, were previously presented by Kepezhinskas et al. (1997) whereas the Ichinsky data represent new analyses. Additionally, as part of this study all the samples were re-analysed by INAA and so the Cs, Zn, Co, Ta, Hf and rare earth elements (REE) represent new data. Insufficient powder was available for full analysis of the Aleutian samples and so the incomplete Aleutian data represent the best that could be patched together from the literature. For the sake of completeness, the full data set is presented in Tables 1–4. The Sr, Nd and Pb isotope ratios were determined statically in multi-collector mode on either a Finnigan MAT 261 or 262 at the Open University. The Sr was fractionation corrected to $^{86}Sr/^{88}Sr = 0.1194$ and Nd to $^{144}Nd/^{146}Nd = 0.7219$. The Pb was analysed in temperature controlled runs (1250 °C) and the ratios corrected for ~1‰ per atomic mass unit mass-fractionation using the recently published recommended values for NBS 981 (Todt et al. 1993). The Sr and Nd isotope ratios were normalised with respect to internally determined values for NBS 987 = 0.71024, and Johnson and Matthey Nd = 0.511850. Measured values over the period of the study were 0.71031 ± 2 and 0.511797 ± 19 (2σ) respectively. Blanks for Sr, Nd and Pb were typically < 1 ng, 200 pg and 300 pg respectively.

Thorium and uranium concentrations and $^{230}Th/^{232}Th$ isotope ratios were determined by thermal ionisation mass spectrometry on a high abundance sensitivity Finnigan MAT 262 equipped with an RPQ-II energy filter. Samples were spiked with a mixed ^{229}Th-^{236}U tracer and dissolved using HF-HCl-HNO_3 in Savillex® beakers. Treatment with HCl and H_3BO_3 was used to obtain completely clear solutions and ensure sample-spike equilibration. Both Th and U concentrations and Th isotope compositions were measured on a single dissolution and a $^{229}Th/^{232}Th$ ratio of ~10^{-3} was aimed for, such that the ^{230}Th contribution from the spike ($^{230}Th/^{229}Th$ ratio of ~10^{-5}) was insignificant in subsequent Th isotope ratio measurements. The $^{230}Th/^{232}Th$ ratios measured on unspiked dissolutions were indistinguishable from those on spiked dissolutions. The Th and U were separated on anionic-exchange resin using HNO_3, HCl and HBr as elutants, and samples were loaded with a HNO_3-H_3PO_4 solution onto double Re filaments, with significant H_3BO_3 remaining from the dissolution. The present procedure is capable of analysing $^{230}Th/^{232}Th$ ratios to 0.5% (1σ) internal precision on as little as 40–60 ng Th. Mass spectrometric procedures follow those described in van Calsteren and Schwieters (1995), and the external reproducibility of this system (~0.5%, 1σ) was monitored using a standard solution (Th'U'std) with a $^{230}Th/^{232}Th$ ratio of 6×10^{-6}, intended to be similar to that of the depleted arc lavas (van Calsteren and Schwieters 1995). Total procedural blanks for U and Th were typically 100 and 50 pg respectively which is negligible compared to the ≥100 ng of sample usually loaded and the error on U/Th ratios is ≤0.5%. Decay constants used in the calculation of activity ratios were the same as those compiled by Goldstein et al. (1989): $\lambda^{230}Th = 9.195 \times 10^{-6}$; $\lambda^{232}Th = 4.948 \times 10^{-11}$; $\lambda^{238}U = 1.551 \times 10^{-10}$. Determinations of the AThO and TML

Table 1 Analyses of lavas from the Eastern Volcanic Front (*LOI* loss on ignition)

Sample	J4668	J4662	C608	J4499	J4497	26107	27077	89012	29M	A4-91	Vil 4-92	G574	M554	C-11217
Locality	Kizimen	Kizimen	M. Semyac	Karymsky	Karymsky	Arik	Aag	Koryaksky	Avachinsky	Avachinsky	Vilyuchinsky	Gorely	Mutnovsky	Ksudach
Distance to trench (km)	210	210	190	195	195	245	220	200	185	185	180	185	170	180
Age	~8300 years	Holocene	< 8000 years	1971 A.D.	1976 A.D.	Late Pleistocene	Mid-Pleistocene	< 7000 years	18–7 ka	1991 A.D.	2000 years	< 600 years	Holocene	1400 years
SiO_2 (wt%)	63.50	55.30	48.80	62.20	62.40	63.50	58.80	52.90	49.10	55.90	58.90	52.30	49.50	50.30
TiO_2	0.57	1.01	0.73	0.86	0.88	0.56	0.77	0.96	1.15	0.85	0.81	1.27	1.21	0.96
Al_2O_3	16.00	17.20	16.50	15.90	15.70	15.40	16.40	17.50	15.50	18.00	16.80	16.70	18.00	18.50
Fe_2O_3	5.27	9.44	11.60	6.33	6.03	5.27	7.43	9.61	10.60	8.30	7.49	11.20	12.00	11.00
MnO	0.13	0.18	0.20	0.16	0.16	0.12	0.15	0.18	0.18	0.16	0.16	0.20	0.20	0.20
MgO	2.25	4.50	9.61	1.98	1.84	2.76	3.79	6.69	9.96	4.17	3.29	4.74	5.46	4.86
CaO	5.49	8.39	9.35	5.24	4.99	5.37	7.43	9.40	10.10	8.64	6.67	9.28	10.70	10.50
Na_2O	3.80	3.14	2.19	4.49	4.58	3.74	3.39	3.19	2.68	3.25	3.83	3.12	2.56	2.40
K_2O	1.72	1.09	0.39	1.59	1.70	1.84	1.41	0.43	0.77	0.65	1.46	0.85	0.38	0.44
P_2O_5	0.15	0.19	0.13	0.25	0.26	0.14	0.18	0.15	0.24	0.15	0.25	0.34	0.18	0.14
LOI	0.05	0.15	0.40	0.15	0.10	0.45	0.15	0.46	0.30	0.00	0.03	0.00	0.15	0.20
Total	98.93	100.59	99.90	99.15	98.64	99.15	99.90	101.47	100.58	100.07	99.69	100.00	100.34	99.50
Cr (ppm)	15	29	99	7	5	62	36	110	727	32	22	98	52	35
Ni	5	13	79	2	2	11	15	46	154	18	11	19	24	18
Sc	13.7	25.5	30.8	19.0	19.5	14.9	22.1	28.2	31.9	24.7	19.7	37.8	39.8	38.6
V	106	254	256	114	101	122	202	242	274	261	184	312	365	353
Rh	36	20	8	20	24	36	22	–	–	21	20	–	–	10
Sr	319	349	365	303	301	372	431	348	456	359	462	444	421	343
Y	18	21	20	30	30	16	19	17.6	19.9	20	21	24.3	22.9	25
Zr	114	84	82	136	139	99	90	66.7	75	70	105	90.3	43.5	41
Ba	665	405	127	401	409	669	516	325	346	301	519	337	171	141
Nb	7	6	4	7	7	5	4	3.8	4.8	4	7	5.2	4.1	2
Cs	1.54	0.83	0.29	0.87	0.98	1.7	0.85	–	0.2	0.75	0.99	0.67	0.4	0.59
Zn	57	109	82	69	77	55	67	80	94	69	59	93	103	84
Co	12.8	23.2	43.8	9.6	9.2	13.5	18.8	30.3	55.4	19.4	17.1	26	31.2	29.8
Tb	0.33	0.23	0.08	0.26	0.28	0.29	0.19	0.11	0.22	0.09	0.26	0.19	0.07	0.06
Hf	3.39	2.54	1.27	4.06	4.17	3.07	2.67	2.23	2.44	2.36	3.10	2.82	1.77	1.75
La	12.0	8.4	4.7	11.7	12.9	11.5	9.9	5.9	7.7	5.9	12.5	11.1	4.6	4.2
Ce	25.4	18.7	9.6	28.5	19.1	23.9	21.4	14.6	18.6	14.3	28.1	25.4	13.3	11.2
Nd	13.7	12.3	8.1	18.9	19.9	12.7	12.6	11.8	13.9	10.7	16.3	16.9	14.6	9.7
Sm	3.19	3.25	2.14	4.65	4.82	2.88	3.16	2.97	3.46	2.97	3.81	4.59	3.65	2.94
Eu	0.97	1.14	0.80	1.39	1.45	0.83	1.00	1.07	1.18	0.99	1.20	1.52	1.31	1.01
Tb	0.52	0.63	0.44	0.84	0.85	0.47	0.55	0.58	0.56	0.64	0.65	0.80	0.80	0.72
Yb	2.09	2.26	1.53	3.16	3.22	1.71	2.03	2.15	2.17	2.29	2.26	2.87	2.80	2.57
Lu	0.33	0.35	0.23	0.50	0.52	0.27	0.32	0.33	0.33	0.36	0.37	0.46	0.40	0.39
Th	2.413	1.312	0.324	1.603	1.692	3.202	2.271	0.751	1.075	0.639	1.646	0.873	0.266	0.563
U	1.339	0.763	0.169	0.968	1.005	1.799	1.133	0.339	0.465	0.349	0.746	0.392	0.125	0.219
$^{87}Sr/^{86}Sr$	0.70332	0.70341	0.70322	0.70320	0.70318	0.70349	0.70340	0.70338	0.70342	0.70338	0.70332	0.70324	0.70331	0.70336
$^{143}Nd/^{144}Nd$	0.513090	0.513049	0.513079	0.513097	0.513139	0.513046	0.513099	0.513035	0.513071	0.513048	0.513065	0.513102	0.513098	0.513073
$^{206}Pb/^{204}Pb$	18.274	18.281	18.368	18.332	18.234	18.334	18.362	18.391	18.34	18.345	18.312	18.329	18.357	18.288
$^{207}Pb/^{204}Pb$	15.477	15.479	15.504	15.465	15.481	15.472	15.492	15.501	15.482	15.492	15.466	15.491	15.502	15.472
$^{204}Pb/^{204}Pb$	37.919	37.933	38.046	37.907	37.853	37.961	38.049	38.106	38.011	38.040	37.973	38.060	38.108	38.007
$(^{230}Th/^{232}Th)$	1.685	1.739	1.646	1.748	1.704	1.739	1.384	1.353	1.357	1.262	1.236	1.317	1.397	1.167
$(^{238}U/^{232}Th)$	1.683	1.765	1.580	1.832	1.802	1.705	1.513	1.369	1.312	1.659	1.375	1.365	1.421	1.182
$(^{230}Th/^{238}Th)$	1.010	0.994	1.051	0.962	0.954	1.029	0.923	0.988	1.034	0.767	0.907	0.965	0.983	0.996

Table 2 Analyses of lavas from the Central Kamchatkan Depression (*LOI* loss on ignition)

Sample	2562	2581/1	2377	3/0B	K-2310	TB-9-7-75	T889	BAK32
Locality	Sheveluch	Sheveluch	Ploskiy	Ploskiy	Kamen	Tolbachik	Tolbachik	Bakening
Distance to trench (km)	200	200	225	225	230	240	240	260
Age	1964 A.D.	Holocene	< 50 ka	< 50 ka	< 50 ka	1975 A.D.	Holocene	~2000 years
SiO_2 (wt%)	58.20	54.40	50.90	49.90	50.50	49.70	50.40	66.00
TiO_2	0.62	0.70	1.70	1.15	1.11	0.92	1.26	0.48
Al_2O_3	16.30	14.60	16.50	14.00	16.80	13.20	13.00	15.85
Fe_2O_3	6.60	8.48	11.20	10.60	10.80	10.20	11.40	4.70
MnO	0.13	0.16	0.18	0.18	0.19	0.19	0.19	0.08
MgO	4.67	8.18	4.87	9.44	7.06	9.65	11.00	1.97
CaO	7.20	8.73	8.11	10.20	10.50	12.10	9.45	4.30
Na_2O	3.87	2.94	3.24	2.44	2.61	2.37	2.35	3.78
K_2O	1.36	1.21	1.77	1.16	0.55	0.75	1.24	2.17
P_2O_5	0.20	0.23	0.53	0.33	0.16	0.18	0.35	0.15
LOI	0.93	0.62	0.30	0.15	0.08	0.62	0.15	0.76
Total	100.08	100.25	99.30	99.55	100.36	99.88	100.79	100.24
Cr (ppm)	213	570	135	534	231	462	764	36
Ni	36	101	46	147	33	98	202	21
Sc	19.4	28.5	24.3	33.8	42.2	42.3	33.4	10.3
V	161	196	327	284	315	284	303	103
Rb	–	–	–	–	–	25	39	43
Sr	648	539	350	303	283	296	314	440
Y	14	14	34.2	22.3	20	18	25	12
Zr	88	67	183	104	56.8	65	115	126
Ba	442	360	492	297	184	263	357	715
Nb	4	2.6	6.4	4.4	3.5	3	3	4
Cs	0.85	0.57	1.48	0.86	–	0.46	0.87	1.32
Zn	64	75	107	89	97	122	115	52
Co	20.8	30.5	30.5	40.2	33.4	39.9	44.6	10.7
Ta	0.15	0.13	0.35	0.21	0.11	0.11	0.23	0.34
Hf	2.78	2.34	4.97	3.11	1.69	1.98	3.25	3.18
La	10.0	7.7	16.4	10.5	4.8	6.5	11.6	13.8
Ce	22.3	18.3	41.0	25.5	12.4	15.0	27.4	26.3
Nd	14.1	11.1	27.7	19.3	12.4	12.1	20.2	12.9
Sm	3.03	2.94	6.62	4.62	3.23	3.32	4.96	2.54
Eu	0.99	0.99	1.87	1.38	1.13	1.09	1.44	0.76
Tb	0.52	0.49	1.06	0.79	0.71	0.61	0.82	0.36
Yb	1.64	1.71	3.65	2.36	2.58	1.87	2.62	1.16
Lu	0.28	0.28	0.58	0.39	0.39	0.29	0.40	0.19
Th	1.228	0.866	1.893	1.031	0.314	0.527	1.134	3.225
U	0.676	0.524	1.153	0.639	0.256	0.338	0.707	1.660
$^{87}Sr/^{86}Sr$	0.70340	0.70339	0.70334	0.70334	0.70351	0.70339	0.70338	0.70338
$^{143}Nd/^{144}Nd$	0.513161	0.513052	0.513123	0.513123	0.513123	0.513111	0.513080	0.513066
$^{206}Pb/^{204}Pb$	18.322	18.368	18.163	18.292	18.292	18.159	18.189	18.330
$^{207}Pb/^{204}Pb$	15.474	15.514	15.453	15.490	15.490	15.486	15.460	15.462
$^{208}Pb/^{204}Pb$	37.885	38.019	37.783	37.913	37.913	37.915	37.826	37.908
$(^{230}Th/^{232}Th)$	1.570	1.646	1.877	1.881	2.344	1.877	1.816	1.552
$(^{238}U/^{232}Th)$	1.671	1.838	1.848	1.880	2.478	1.948	1.891	1.562
$(^{230}Th/^{238}U)$	0.940	0.895	1.016	1.000	0.946	0.972	0.968	1.002

Th standards yielded $(^{230}Th/^{232}Th) = 1.017 \pm 0.005$ ($n = 5$) and $(^{230}Th/^{232}Th) = 1.079 \pm 0.005$ ($n = 2$) during this period. The U-Th isotope data determined using the α-counting method on three of the Aleutian samples (Newman et al. 1984) and lavas from Avachinsky and Tolbachik in Kamchatka (Chabaux and Allègre 1994) are within analytical error of the new mass spectrometric data.

Results

Major and trace elements

The analysed lavas range from high-MgO, low-K_2O tholeiitic basalts and basaltic andesites through to calc-alkaline andesites, dacites and rhyolites (Fig. 2a). The Mg# [$Mg/(Mg + 0.85 \times Fe_{total})$] typically ranges from 0.42 to 0.55, however 6 lavas (2581/1, C608, 29 M, 3OB, T889 and TB-9–7-75) have Mg# = 0.66–0.69 and contain $Fo_{83–65}$ olivines (Kepezhinskas et al. 1997) and are thus close to being primary melts in equilibrium with mantle peridotite. On diagrams of K_2O versus SiO_2 and MgO (Fig. 2a, b), the EVF lavas form a coherent array and although the CKD lavas exhibit a similar trend they show more scatter. The increase in K_2O with increasing SiO_2 and decreasing MgO suggests that crystal fractionation is the dominant control on the variation in K_2O within both the EVF and CKD lava suites (e.g. Kersting and Arculus 1994; Hochstaedter et al. 1996). However, it is noteworthy that the CKD lavas are displaced overall from the EVF to higher K_2O even at low

Table 3 Analyses of lavas from Ichinsky volcano (*LOI* loss on ignition)

Sample	ICH-183	ICH-2200	ICH-50062
Locality	Ichinsky	Ichinsky	Ichinsky
Distance to trench (km)	380	380	380
Age	< 40 ka	< 40 ka	< 40 ka
SiO_2 (wt%)	55.66	56.61	56.56
TiO_2	1.52	0.67	0.62
Al_2O_3	17.65	17.36	17.88
Fe_2O_3	7.90	7.62	7.31
MnO	0.21	0.17	0.17
MgO	2.59	3.66	2.85
CaO	4.93	8.57	6.98
Na_2O	5.29	3.21	3.45
K_2O	2.76	0.92	1.40
P_2O_5	1.03	0.20	0.21
LOI	0.16	0.96	2.45
Total	99.70	99.95	99.88
Cr (ppm)	8	36	9
Ni	2	12	12
Sc	10.0	24.0	14.0
V	52	194	152
Rb	31	13	27
Sr	739	596	589
Y	43	19	20
Zr	335	74	97
Ba	977	467	586
Nb	35	1	3
Cs	0.41	0.31	–
Zn	106	69	60
Co	8	18	16
Ta	2.05	0.08	–
Hf	6.81	2.22	2.48
La	44.2	8.5	11.5
Ce	91.4	19.8	25.0
Nd	47.8	13.5	15.0
Sm	9.54	3.27	3.36
Eu	2.94	1.08	1.08
Tb	1.25	0.51	0.48
Yb	3.54	1.96	1.87
Lu	0.53	0.31	0.30
Th	4.301	0.644	1.403
U	1.114	0.330	0.526
$^{87}Sr/^{86}Sr$	0.70339	0.70339	0.70335
$^{143}Nd/^{144}Nd$	0.512945	0.513122	0.513055
$^{206}Pb/^{204}Pb$	18.131	18.333	18.270
$^{207}Pb/^{204}Pb$	15.462	15.429	15.448
$^{208}Pb/^{204}Pb$	37.871	37.836	37.905
$(^{230}Th/^{232}Th)$	0.795	1.587	1.210
$(^{238}U/^{232}Th)$	0.786	1.554	1.137
$(^{230}Th/^{238}U)$	1.011	1.021	1.064

SiO_2 and high MgO indicating different, more potassic parental magmas. Two of the Ichinsky samples plot amongst the EVF and CKD lavas, whereas a dacite has high K_2O along with one CKD lava and the dacite from Bogoslof in the Aleutians. The few other lavas analysed from the Aleutians lie amongst the EVF and CDK lavas.

Incompatible trace element concentrations are quite high overall when compared with low-K arc lavas such as those from Tonga (e.g. Ewart and Hawkesworth 1987; Turner et al. 1997). The lavas form typical island arc patterns on mantle normalised, multi incompatible-element diagrams (Fig. 3). The large ion lithophile elements (LILE), including Sr, are enriched over the high field strength elements (HFSE) which form prominent troughs at Th, Ta, Ti and to a lesser extent Zr. The rare earth elements (REE) show light REE enrichment and with the exception of the three high-K lavas, the Kamchatka data have relatively constant Ce/Yb over the range MgO = 11–2% (Fig. 2c) and all fall within the low Ce/Yb group (i.e. Ce/Yb < 15) of Hawkesworth et al. (1991).

The compositions of the average sediment being subducted on the Pacific plate beneath Kamchatka (AKS) and the Aleutians (AAS) calculated by Plank and Langmuir (1998) are also plotted on Fig. 3. A striking observation is that these have incompatible element abundances that are very similar to those of the average CKD, EVF and Aleutian lavas mirroring their patterns, including the negative Ta anomaly, in Fig. 3. Exceptions are the higher Th concentrations and prominent trough at Zr-Hf observed in the average sediment. Although the data set presented here do not include Pb concentration data, analyses given by Kersting and Arculus (1995) ranged from 2.2–5 ppm Pb which is significantly less than the 10 ppm Pb in the average sediment (Plank and Langmuir 1998).

Sr, Nd and Pb isotopes

The isotope data are shown in Fig. 4. On the $^{143}Nd/^{144}Nd$ versus $^{87}Sr/^{86}Sr$ diagram the CKD and EVF lavas are tightly clustered with $^{143}Nd/^{144}Nd$ ratios that range from 0.51316 to 0.51298 and $^{87}Sr/^{86}Sr$ ratios that range from 0.7033 to 0.7035. In detail, there is an overall shallow negative trend, particularly well developed in the EVF lavas (see inset in Fig. 4). Such $^{143}Nd/^{144}Nd$ values are unusually high for island arc rocks and require a source which has had a long term depletion of incompatible trace elements similar to the mid-ocean ridge basalt (MORB) source. Most island arc rocks are less isotopically depleted than MORB, but the Kamchatka lavas are an exception to this. In Fig. 4 they overlap the field for Pacific MORB in terms of $^{143}Nd/^{144}Nd$ but at slightly higher $^{87}Sr/^{86}Sr$ values. Note that the average sediment subducted beneath Kamchatka has $^{143}Nd/^{144}Nd = 0.51234$ and $^{87}Sr/^{86}Sr = 0.7112$. There is little evidence for any systematic difference in Sr or Nd isotopes between the EVF and CKD lavas. Finally, the Aleutian samples are indistinguishable from the Kamchatka data in terms of their $^{87}Sr/^{86}Sr$ ratios but are clearly displaced to lower $^{143}Nd/^{144}Nd$ (0.51299–0.51271). Excepting the low $^{87}Sr/^{86}Sr$ for the lava from Bogoslof, the Aleutian lavas define a negative array with a much steeper slope than that for the Kamchatka data.

Kersting and Arculus (1995) showed that the Pb isotope composition of lavas from Klyuchevskoy volcano from the CKD were amongst the least radiogenic island arc lavas yet measured. The larger data set presented here and by Kepezhinskas et al. (1997) confirm and expand this result. The CKD and EVF lavas

Table 4 Analyses of lavas from the Aleutians

Sample	UM21	KAN 5-8	K81-7A	SAR 7[a]	BOG 1796	ADAG-81DR[c]	MM 77-102[c]
Locality	Umnak	Kanaga	Kasatochi	Unimak	Bogoslof	Adak	Adak Mt Moffett
Age (y)	1946	1900	Active	Active	1796	Quaternary	Quaternary
SiO_2 (wt%)	52.24	53.65	49.07	50.20	61.00	48.46	–
TiO_2	1.09	0.68	0.66	1.38	0.53	0.69	–
Al_2O_3	17.62	17.68	15.75	18.35	18.60	15.14	–
Fe_2O_3	10.78	7.85	9.80	12.21	4.70	9.03	–
MnO	0.15	0.18	0.14	0.17	0.07	0.21	0.13
MgO	4.97	5.51	8.77	4.27	1.10	11.83	–
CaO	10.80	8.39	12.52	10.42	6.50	11.37	–
Na_2O	2.91	3.38	2.24	3.33	4.08	2.08	1.65
K_2O	0.66	1.71	0.76	0.77	2.90	0.74	–
P_2O_5	–	–	0.15	0.00	0.28	–	–
Total	101.22	99.03	99.86	101.10	99.76	99.55	–
B (ppm)	17	32	11	13	15	–	–
Cr	62	21	338	30	5	3700	1494
Ni	17	9	61	9	3	233	–
Sc	43	24	45	38	5	88	60
Rb	16	–	12	29	129	0	5
Sr	360	–	482	400	730	31	246
Zr	–	109	–	–	166	–	–
Ba	204	471	228	281	1725	6	–
Cs	1	2.55	0.56	0.96	4.8	0.1	0.59
Ta	0.26	0.17	0.10	0.28	5.30	0.01	–
Hf	2.06	3.00	1.30	2.80	0.47	0.11	1.13
La	6.4	10.2	5.4	9.4	26.6	0.2	3.6
Ce	16.6	24.4	13.6	24.4	62.2	0.8	9.4
Nd	10.9	12.8	7.7	12.3	27.1	1.3	7.8
Sm	2.92	3.65	2.34	4.19	5.71	0.52	2.40
Eu	1.04	1.03	0.65	1.42	1.48	0.20	0.72
Tb	0.61	0.60	0.42	0.77	0.58	0.10	0.36
Yb	2.22	2.51	1.49	2.87	2.31	0.26	0.87
Lu	0.31	0.34	0.22	0.39	0.32	0.04	0.15
Th	1.174	3.497	1.078	1.930	4.814	0.017	1.130
U	0.610	1.647	0.617	0.836	2.112	0.006	0.383
$^{87}Sr/^{86}Sr$	0.70330	0.70332	0.70336	0.70335	0.70314	0.70336	0.70323
$^{143}Nd/^{144}Nd$	0.512987	0.512956	0.512916	0.512926	0.512917	0.512215	0.512911
$^{206}Pb/^{204}Pb$	18.813	18.770	18.873	18.854	18.832	18.344	18.591
$^{207}Pb/^{204}Pb$	15.533	15.529	15.561	15.555	15.566	15.526	15.525
$^{208}Pb/^{204}Pb$	38.282	38.243	38.384	38.361	38.329	37.882	38.083
$(^{230}Th/^{232}Th)$	1.286	1.243	1.288	1.313	1.292	–	1.345
$(^{238}U/^{232}Th)$	1.576	1.429	1.737	1.314	1.331	1.112	1.029
$(^{230}Th/^{238}U)$	0.823	0.878	0.748	1.008	0.979	–	1.318
B/Be[b]	31.5	39.0	26.2	21.3	5.9	–	–
$^{10}Be/^{9}Be$[b]	7.5	10.6	14.6	6.1	9.0	–	–

[a] Pb and Sr isotope data are from SAR 18
[b] B and Be isotope data from Morris et al. (1990)
[c] Samples ADAG-81DR and MM 77-102 are xenoliths from Adak island

straddle the northern hemisphere reference line (NHRL) on the $^{207}Pb/^{204}Pb$ versus $^{206}Pb/^{204}Pb$ diagram (Fig. 4) and lie within and at the low $^{206}Pb/^{204}Pb$ end of the Pacific MORB field. The lavas lie slightly above the NHRL in terms of their $^{208}Pb/^{204}Pb$ ratios but still overlap the Pacific MORB field. As with the Sr and Nd isotope data, there is little evidence for any distinction between the EVF and CKD lavas, although the EVF lavas form a positive array on both Pb-isotope diagrams. In contrast to the Kamchatka data, the Aleutian lavas are strongly displaced to higher $^{206}Pb/^{204}Pb$ ratios. Although some rocks from the Aleutians extend above the NHRL to higher $^{208}Pb/^{204}Pb$ and $^{207}Pb/^{204}Pb$, partly overlapping the Pb isotope range of the sediments (Kay et al. 1978), those included in this study have lower $^{208}Pb/^{204}Pb$ and $^{207}Pb/^{204}Pb$ than the sediments and so still straddle the NHRL (see Fig. 4).

U-Th isotopes

Kamchatka

The U-Th isotope results are presented on a $(^{230}Th/^{232}Th)$ versus $(^{238}U/^{232}Th)$ equiline diagram in Fig. 5. The Kamchatka lavas show a very large range in $(^{238}U/^{232}Th)$ (2.48–0.79) similar to the Lesser Antilles (Turner et al. 1996) and Marianas (Elliott et al. 1997) arcs. However, in contrast to these other island arcs, the majority lie on or just to the right of the equiline with

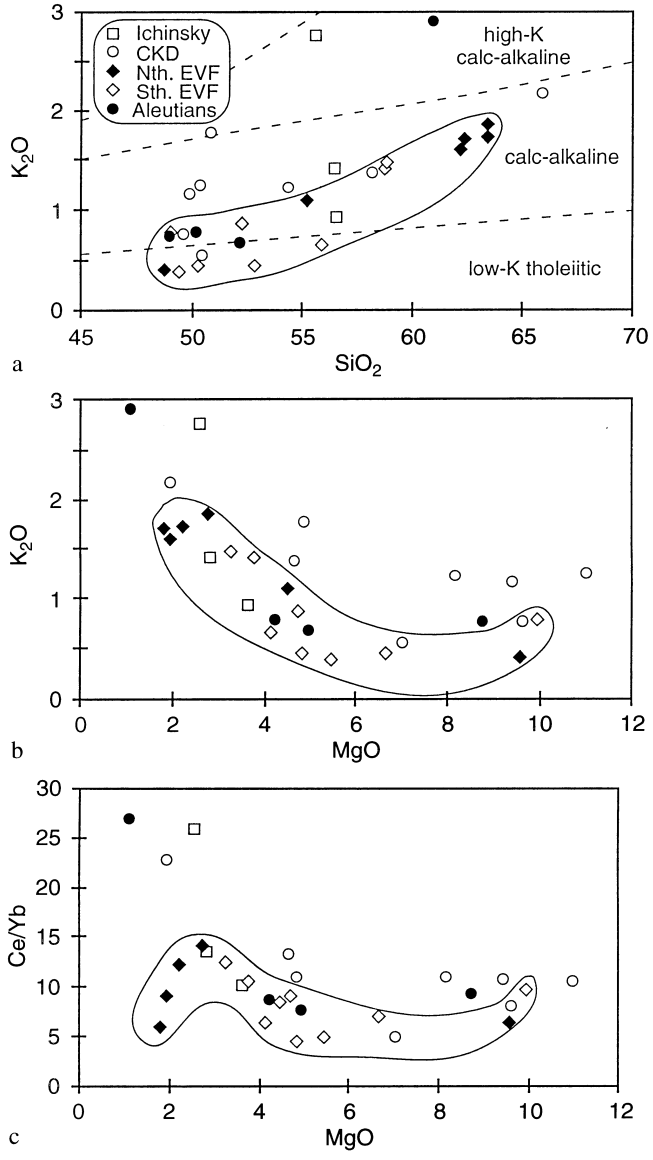

Fig. 2a-c K_2O versus SiO_2, (**a**), MgO (**b**), and Ce/Yb versus MgO (**c**) illustrating the compositional range of the lavas analysed. The EVF lavas (*highlighted* with an *outline field* and subdivided into a northern and southern group as described in Fig. 1) form a relatively coherent array extending from low-K tholeiitic basalts and basaltic andesites through to calc-alkaline andesites, dacites and rhyolites whereas the CKD lavas show more scatter and apparently evolved from higher-K parental magmas. Ce/Yb remains relatively constant and < 15 over the range of MgO, the CKD lavas possibly having higher Ce/Yb parental magmas

minor ^{238}U excesses leading to a correspondingly large range in ($^{230}Th/^{232}Th$). Similar results have been obtained by Churikova et al. (1997).

In detail, the CKD lavas have high ($^{230}Th/^{232}Th$) and ($^{238}U/^{232}Th$) > 1.6 and three samples lie on or within analytical error of the equiline while the remaining five have ^{238}U excesses ranging from 3–10%. The sample from Kamen volcano lies well apart from the rest of the lavas with ($^{230}Th/^{232}Th$) = 2.34 and ($^{238}U/^{232}Th$) = 2.48. The northern and southern subgroups of the EVF lavas can be distinguished on the basis of their U/Th, ($^{238}U/^{232}Th$) and ($^{230}Th/^{232}Th$) ratios. Those south of the influence of the CKD (Aag-Ksudach) have low U/Th and ($^{230}Th/^{232}Th$) (1.17–1.38) and extend from the equiline out to the right with up to 23% ^{238}U excesses. In contrast, the northern EVF volcanoes, adjacent to the CKD, have much higher U/Th and ($^{230}Th/^{232}Th$) ratios of (1.58–1.83) overlapping those of the CKD lavas to their west (Fig. 1) and these tend to be closer to secular equilibrium with ($^{230}Th/^{238}U$) = 0.92–1.03. The three lavas from Ichinsky show a large range in both ($^{230}Th/^{232}Th$) and ($^{238}U/^{232}Th$), but are most akin to the southern EVF lavas with ($^{230}Th/^{232}Th$) = 0.78–1.59 and have 1–6% ^{230}Th excesses, although two are essentially within error of the equiline.

Aleutians

The Aleutian lavas show a much more restricted range in ($^{230}Th/^{232}Th$) (1.24–1.35) than the Kamchatka data but exhibit a large range in U-Th disequilibrium. The xenolith from Mt. Moffatt on Adak island that was analysed for its Th isotope composition has a 32% ^{230}Th excess, whereas the five lavas form an array extending from the equiline out to the right with up to 25% ^{238}U excesses.

Isotope ^{10}Be is cosmogenic with a half life of 1.5 million years that is highly enriched in oceanic sediments. The five Aleutian lavas were analysed for their B concentration and $^{10}Be/^{9}Be$ ratios by Morris et al. (1990) and these data are reproduced in Table 4. All contain significant concentrations of ^{10}Be ($^{10}Be/^{9}Be$ ranges from 6.1 to 14.6×10^{-11}) and B (4–32 ppm) although there is little or no correlation between $^{10}Be/^{9}Be$ and B/Be for these lavas. In contrast, the Kamchatka lavas do not have elevated ^{10}Be ($^{10}Be/^{9}Be$ = 1 to 4×10^{-11}, Tera et al. 1990). One of the objectives of analysing the Aleutian lavas in the present study was to investigate any covariation with U-Th isotopes. In the New Britain arc, for example, Gill et al. (1993) found a positive correlation between $^{10}Be/^{9}Be$ and ($^{230}Th/^{232}Th$), but no correlation with ^{238}U-excess. In contrast, Fig. 6 shows that the Aleutian lavas show little correlation or possibly even a negative correlation between $^{10}Be/^{9}Be$ and ($^{230}Th/^{232}Th$) but a positive relationship between $^{10}Be/^{9}Be$ and U-excess [i.e. ($^{238}U/^{230}Th$) > 1]. Sigmarsson et al. (1990) have observed a similar correlation in Andean lavas.

Discussion and interpretation

Trace element and radiogenic isotope variations

The depletion of Ta (and Nb) relative to the LREE is a characteristic of island arc lavas and so the behaviour of the La/Ta ratio with MgO is investigated in Fig. 7a. In

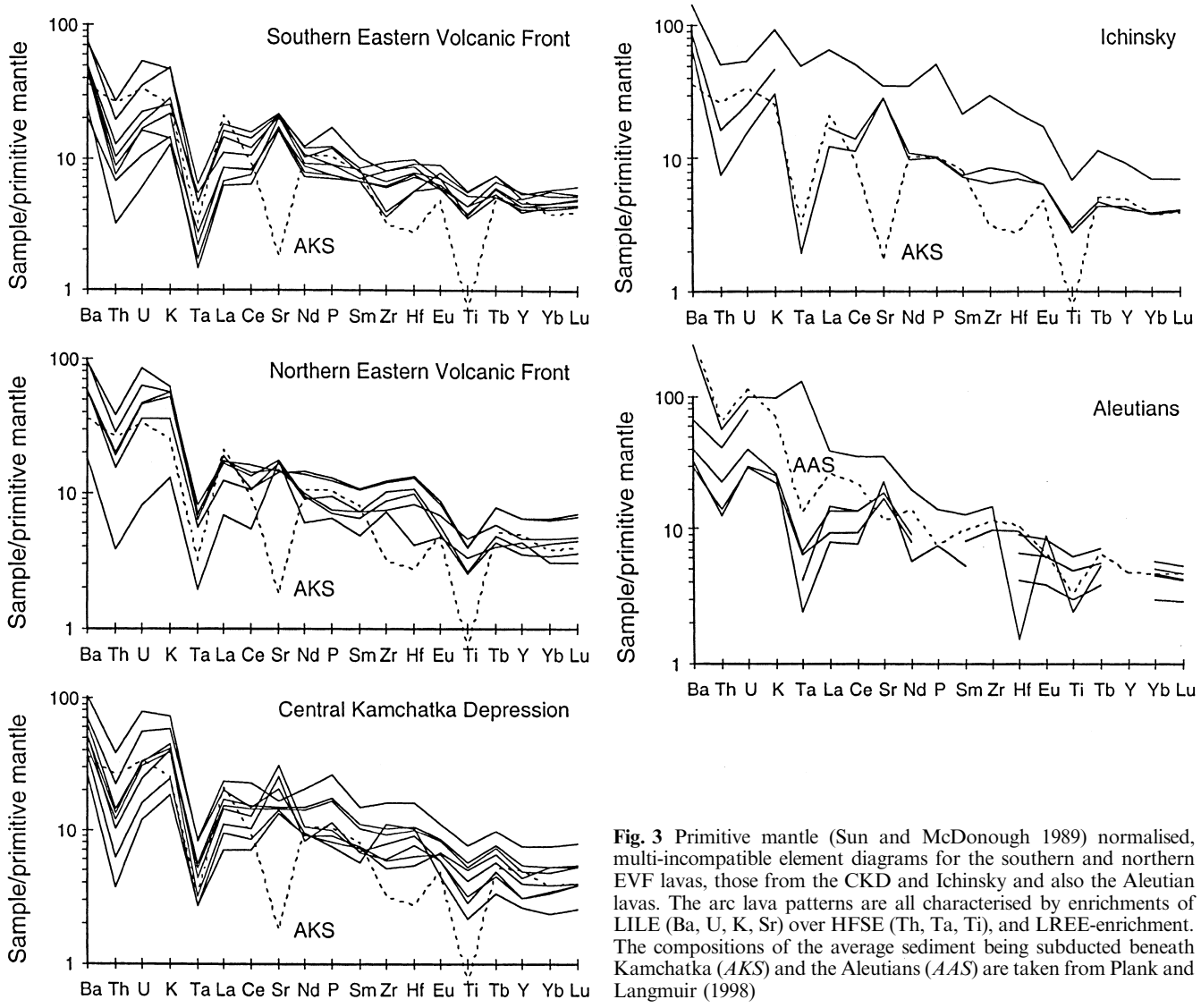

Fig. 3 Primitive mantle (Sun and McDonough 1989) normalised, multi-incompatible element diagrams for the southern and northern EVF lavas, those from the CKD and Ichinsky and also the Aleutian lavas. The arc lava patterns are all characterised by enrichments of LILE (Ba, U, K, Sr) over HFSE (Th, Ta, Ti), and LREE-enrichment. The compositions of the average sediment being subducted beneath Kamchatka (*AKS*) and the Aleutians (*AAS*) are taken from Plank and Langmuir (1998)

the high-MgO rocks, La/Ta is relatively constant, however below MgO = 6% La/Ta decreases and also shows more scatter. In Fig. 7b, there is a positive array between La and Ta indicating that both elements are behaving incompatibly, however Ta increases more rapidly at high concentrations than La. The simplest interpretation is that the decrease in La/Ta below 6% MgO reflects crystal fractionation where Ta is somewhat more incompatible than La. That the majority of the La/Ta variation reflects shallow level crystal fractionation processes rather than source variations is supported by the observation that there is no correlation between La/Ta and $^{207}Pb/^{204}Pb$ or $^{143}Nd/^{144}Nd$ (Fig. 8). A similar observation can be made for other REE and HFSE ratios, for example Ce/Yb is relatively constant in the high-MgO rocks, most of the variation in this ratio also occurs at MgO < 6% (Fig. 2c) with Ce/Yb increasing as La/Ta decreases. In a detailed study of Klyuchevskoy volcano, Kersting and Arculus (1994) have shown that compositional variation is dominated by crystal fractionation with more minor effects resulting from magma chamber recharge.

In addition to negative Ta-Nb anomalies, island arc rocks are also characterised by enrichments of LILE elements such as Ba, U and Pb relative to the HFSE or REE (e.g. Gill 1981; Pearce 1982; Hawkesworth et al. 1993). Figure 9 shows that the Ba/Th ratios of the Kamchatka rocks are much higher than those of MORB or sediment and extend up to values of 700. The Ba/Th shows no correlation with MgO (not shown) and so the data appear to require the addition of a high Ba/Th component. However, as with La/Ta, the range in Ba/Th occurs at relatively constant $^{87}Sr/^{86}Sr$, and whilst there is more scatter Ba/Th versus $^{206}Pb/^{204}Pb$ also shows no correlation (Fig. 9). Finally, the U/Th ratios range from 0.2 to 0.8 and are generally much higher than that for either N-MORB (0.4) or OIB (0.3) (Sun and McDonough 1989). They show a mild decrease with decreasing MgO and increasing Ce/Yb (not shown). The Sr, Nd and Pb isotope ratios do not appear to vary with U/Th.

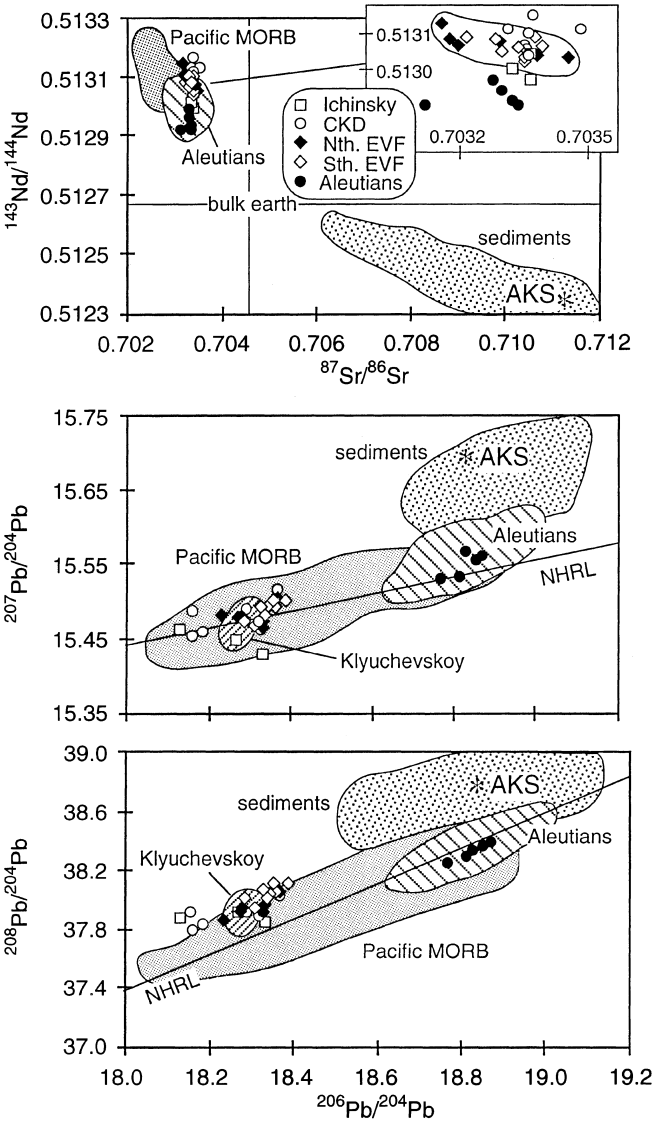

Fig. 4 Conventional Sr, Nd and Pb isotope diagrams showing that with the exception of slightly elevated $^{87}Sr/^{86}Sr$, the Kamchatka lavas are essentially indistinguishable from Pacific MORB (data from White et al. 1987). Pb isotope field for Klyuchevskoy taken from Kersting and Arculus (1995). In contrast, the Aleutian lavas are significantly displaced to lower $^{143}Nd/^{144}Nd$ and along the NHRL to higher $^{208}Pb/^{204}Pb$, $^{207}Pb/^{204}Pb$ and $^{206}Pb/^{204}Pb$ in the direction of the subducting sediments (data from Kay and Kay 1988; McDermott and Hawkesworth 1991; Kersting 1995; average (*AKS*) from Plank and Langmuir 1998). Error *bars* are generally smaller than the symbol size

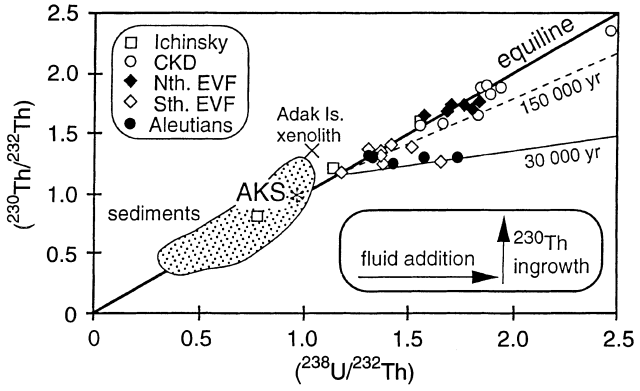

Fig. 5 $(^{230}Th/^{232}Th)$ versus $(^{238}U/^{232}Th)$ equiline diagram for Kamchatka and Aleutian lavas. The majority of the Kamchatka lavas lie on the equiline or just to the *right* of the equiline with minor ^{238}U-excesses. Nevertheless, they have a large range in U/Th ratios extending to quite high $(^{238}U/^{232}Th)$, and a correspondingly large range in $(^{230}Th/^{232}Th)$. Several of the Aleutian lavas and one from the EVF lie well to the *right* of the equiline, having quite large ^{238}U-excesses. A 30 thousand year reference line is drawn through these data. The *inset* illustrates the interpretation for the majority of the Kamchatka lavas implying >150 thousand years has elapsed since fluid release from the slab (see text for discussion). Error *bars* are generally smaller than the symbol size

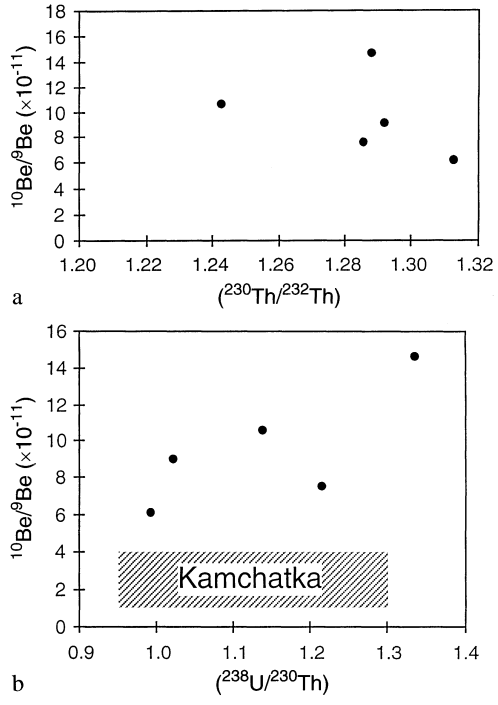

Fig. 6a,b $^{10}Be/^{9}Be$ versus: **a** $(^{230}Th/^{232}Th)$; and **b** $(^{238}U/^{230}Th)$ for the five Aleutian lavas. Although largely controlled by one point, the apparent positive correlation with $(^{238}U/^{230}Th)$ suggests that although the ^{10}Be must originally derive from the upper parts of the subducted sediment pile, it is transported into the mantle wedge by fluids inferred to be derived from the altered oceanic crust as they pass through the sediments. The *shaded bar* indicates the range for Kamchatka lavas (data from Tera et al. 1990)

In summary, there is little or no correlation between incompatible trace element ratios and radiogenic isotopes (Figs. 8 and 9). Much of the variation in ratios such as La/Ta appears to reflect crystal fractionation and the parental magma La/Ta ratio is best estimated from that of the high-MgO rocks that approach primary melts; for these La/Ta is relatively constant at around 50–68. Such ratios are significantly higher than those for N-MORB or OIB (19 and 14 respectively, data from Sun and McDonough 1989) and whilst this might be explained by addition of a sediment component, the striking feature of the Kamchatka rocks is that in terms of their Nd and Pb (and to a lesser extent Sr) isotopes, they are as isotopically depleted as Pacific MORB

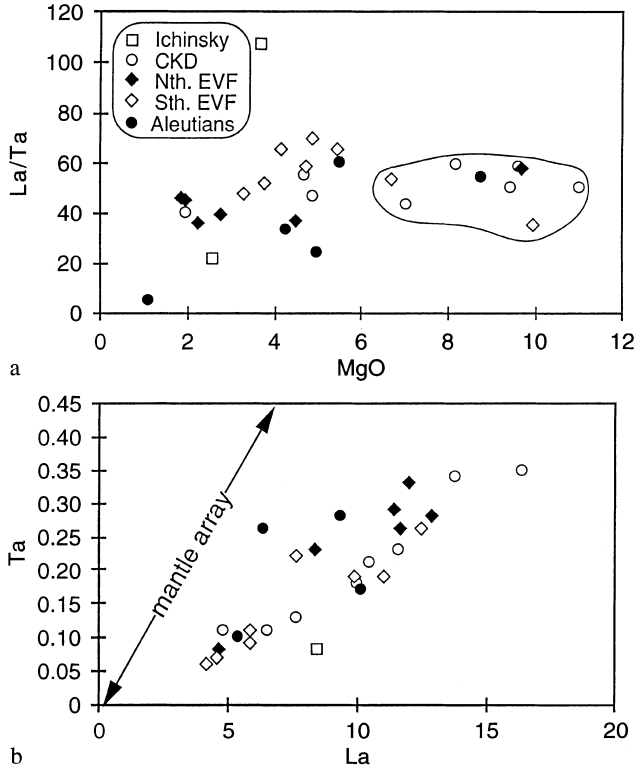

Fig. 7 **a** La/Ta versus MgO showing that much of the observed variation in La/Ta occurs at MgO < 6% and presumably reflects shallow level, closed system processes since there is no associated change in radiogenic isotopes (see Fig. 8). **b** Ta versus La where the Kamchatka rocks show a broad positive trend indicating that both La and Ta are behaving incompatibly. Note, however, that at higher concentrations Ta increases more rapidly than La hence the drop in La/Ta at low MgO in **a**

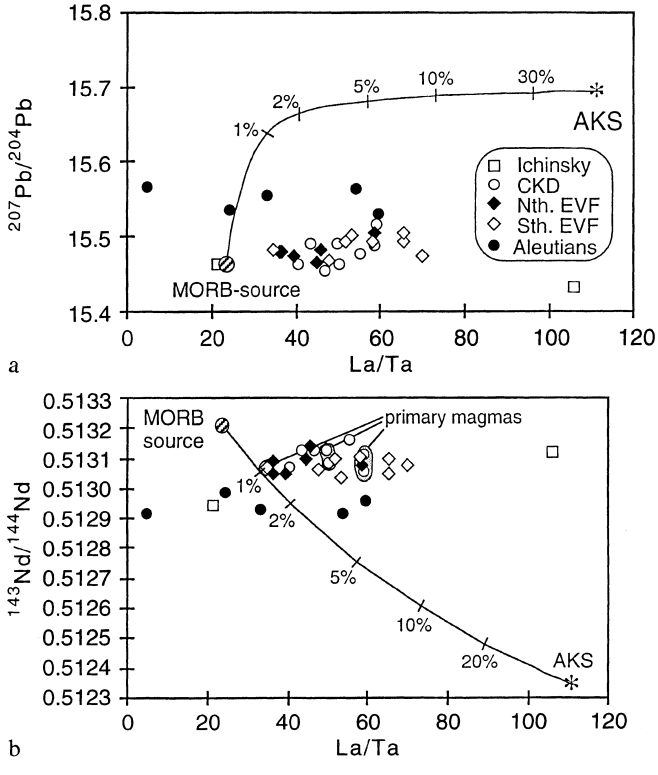

Fig. 8a,b La/Ta versus: **a** $^{207}Pb/^{204}Pb$; **b** $^{143}Nd/^{144}Nd$ with mixing lines between a MORB source and subducted sediment suggesting that little or no sediment is incorporated in the source of the Kamchatka lavas. A maximum of 1% can be accommodated by the Nd isotope data if it is assumed that the Pb isotopes have been modified by fluid addition (see Fig. 9). This contrasts with the ~5% sediment contribution that would be required to produce a source with a La/Ta ratio of 50–68 as found in the high-MgO lavas (cf Fig. 7). End-member compositions used in the mixing calculations were the MORB source of Stolper and Newman (1994), with $^{207}Pb/^{204}Pb$ and $^{143}Nd/^{144}Nd$ ratios appropriate to a Pacific MORB source being taken from Fig. 4 to be 15.45 and 0.5132 respectively, and the average sediment subducting beneath Kamchatka from Plank and Langmuir (1998)

(Fig. 4). At face value, this would appear to conflict with models in which the characteristic arc trace element signature reflects addition of isotopically enriched material from the subducting slab to the mantle wedge. Finally, the data also require the addition of a high LIL/HFSE component. The following sections endeavour to constrain the potential source components and their relative contributions.

The composition of the mantle wedge

The mantle wedge beneath some island arcs has been depleted by back arc melt extraction as inferred from very low incompatible trace element concentrations (particularly the HFSE and REE) in the arc lavas which additionally renders them highly sensitive to the addition of fluids and sediments from the subducting slab (e.g. the Tonga arc, Ewart and Hawkesworth 1987; Turner et al. 1997). Hochstaedter et al. (1996) and Churikova et al. (1997) have suggested that some of the EVF Kamchatka lavas were derived from a source which had undergone depletion by previous melt extraction by back arc volcanoes in the CKD, however if such depletion has occurred then its observable effects are relatively minor compared with Tonga, for example. The Nd and Pb isotope data indicate that the Kamchatka lavas were derived from a source similar to that of Pacific MORB and there is a slight suggestion in Fig. 2c that the EVF lavas had lower Ce/Yb parental magmas than the CKD lavas, though there is no correlation with $^{143}Nd/^{144}Nd$ (cf. Fig. 4). However, the lavas are all LREE-enriched with chondrite normalised $Ce/Yb_n > 1.1$ ($Ce/Yb > 5$ in Fig. 2) and the majority (19 out of 25) also have primitive mantle normalised $Ta/Yb_n \geq 1$, the exceptions being Mutnovsky, Ksudach, Kamen, Malyi Semyachik, Koryaksky and one lava from Avachinsky in which Ta/Yb_n ranges from 0.3 to 0.7. Thus, even if these latter lavas were derived from previously depleted sources there appears to be no systematic spatial control on their distribution. One possibility is that the regional shift to higher U/Th observed in the CKD lavas (cf. Fig. 5) and those from the northern EVF in front of the CKD reflects a mantle

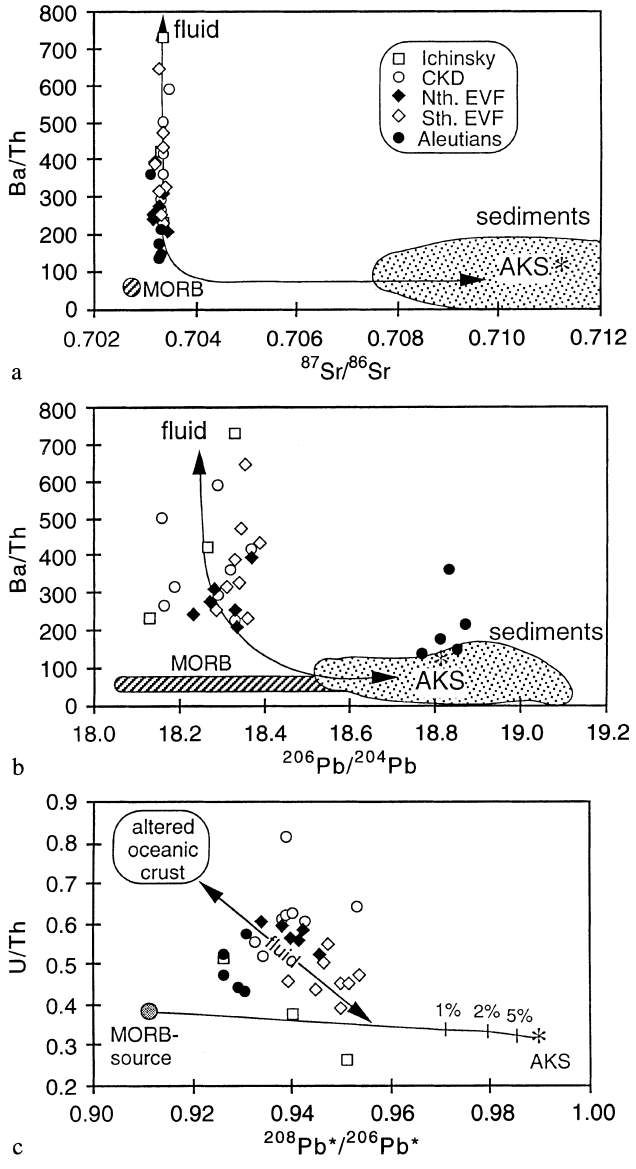

Fig. 9a-c Ba/Th versus: **a** $^{87}Sr/^{86}Sr$; **b** $^{206}Pb/^{204}Pb$ in which the high Ba/Th ratios are taken as indicative of a fluid component which the Sr and Pb isotope data suggest must be derived from altered oceanic crust rather than the subducting sediments. In **c**, U/Th is plotted against the radiogenic $^{208}Pb^*/^{206}Pb^*$ (after Allègre et al. 1986). Altered oceanic crust has high U and Pb contents and U/Th and $^{208}Pb^*/^{206}Pb^*$ ratios and so departures from wedge – sediment mixing lines (mixing parameters as for Fig. 8) towards high U/Th and $^{208}Pb^*/^{206}Pb^*$ are interpreted to reflect addition of fluids derived from the altered oceanic crust in the down-going plate (Turner et al. 1997). The corollary is that the development of U/Th ratios consistently higher than those for MORB or OIB, reflects fluid addition and thus the extension of the Kamchatka data along the equiline in Fig. 5 reflects fluid addition and subsequent ^{230}Th-ingrowth

wedge previously depleted by the Sredinny Ridge volcanoes, however there is no negative correlation between U/Th and Ta/Yb as might be expected if this were the case. We conclude that there is little evidence for the mantle source of the EVF lavas being markedly more depleted than that of the CKD lavas or Pacific MORB and that this is consistent with the lack of significant back arc spreading (splitting of the arc along the CKD is still in its infancy). Finally, we note that none of the EVF or CKD lavas have Sr/Y > 40 or are depleted in the HREE suggesting that garnet was not a residual phase during partial melting. This contrasts with the lavas from the northern segment where Sr/Y ratios often exceed 40 and Nb anomalies can be absent (Kepezhinskas et al. 1997; Volynets et al. 1997). These features have been used to infer a contribution from partial melts of the subducting slab which is young and hot in this region (Kepezhinskas et al. 1997; Volynets et al. 1997). There is no similar evidence for a contribution from slab melts in the EVF and CKD lavas we have investigated.

The contribution from subducted sediments

One of the important questions regarding the petrogenesis of the Kamchatka lavas is whether or not they contain a contribution from subducted sediment which could help to explain features like their negative Ta-Nb anomalies. If La/Ta is essentially unmodified by partial melting (but see below), then the La/Ta ratio of the source of the Kamchatka lavas must be similar to that of the high-MgO lavas (La/Ta = 50–68). On the basis of Pb isotopes, Kersting and Arculus (1995) suggested that little or no sediment had been added to the source of the Kamchatka lavas and this would be consistent with the absence of a ^{10}Be signal (Fig. 6, but see discussion below). The Pb argument is illustrated in Fig. 8a where a MORB source (taken from Stolper and Newman 1994)–sediment mixing curve is shown on a plot of $^{207}Pb/^{204}Pb$ versus La/Ta. Because sediments have high $^{207}Pb/^{204}Pb$ and Pb concentrations, diagrams such as that shown in Fig. 8a are sensitive to sediment addition. As the diagram shows, to obtain La/Ta ratios of 50–68 by addition of sediment to the source of the lavas requires addition of ~5% sediment yet the Pb isotopes permit essentially no sediment addition. One potential problem in the use of Pb isotopes as a tracer of sediments in subduction zone rocks is that Pb is highly mobile in fluids (e.g. Brenan et al. 1995; Keppler 1996) and may also be derived by dehydration of the subducting oceanic crust (e.g. Miller et al. 1994; Turner et al. 1996, 1997). The REE are far less mobile in aqueous fluids (e.g. Keppler 1996) and upper crustal sediments are LREE enriched, therefore Nd isotopes arguably provide a more robust tracer of sediment addition in arc lavas (e.g. Hawkesworth et al. 1997b). Figure 8b shows the same MORB source – sediment mixing curve on a $^{143}Nd/^{144}Nd$ versus La/Ta diagram. Unlike the Pb isotope data, the Nd isotope data will allow some sediment addition (~1%) due to the low Nd concentration in the average sediment being subducted beneath Kamchatka (14 ppm, Plank and Langmuir 1998). However, it is important to note that individual sediment analyses from the north Pacific range up to 213 ppm Nd (Kay and Kay 1988) and so if

an average of 90 ppm Nd is used then very little sediment addition is permitted consistent with the Pb isotope constraints (i.e. 1% is an upper limit).

A potential problem with the simple mixing calculations just described is that they are end-member calculations in as much as they assume addition of bulk sediment. Addition of a partial melt of sediment is more probable, and several recent studies have argued that the sediment component is required to be a highly fractionated partial melt, possibly in equilibrium with residual rutile (Turner et al. 1996; Elliott et al. 1997; Plank and Johnson 1997). However, whilst a sediment melt may have an elevated La/Ta ratio it can also be expected to have higher Nd and Pb concentrations. This means that mixing curves on Fig. 8b remain strongly convex downwards and cannot replicate the essentially horizontal data array irrespective of the La/Ta ratio of the sediment end-member. The problem therefore remains that even if a maximum sediment addition of 1% is assumed, the resultant source La/Ta is ~30 yet the primitive lavas have measured ratios of 50–68.

One possible solution is addition of a high La/Ta component with MORB-like isotope ratios. This could be achieved either through addition of volcaniclastic sediments or if the subducted sediments undergo considerable isotopic equilibration with the mantle wedge via scavenging of Pb and Nd (e.g. Hawkesworth et al. 1993). However, the sediment package on the subducting Pacific plate adjacent to Kamchatka contains only a very minor volcaniclastic component (Rea 1993) and it seems unlikely that wholesale isotopic equilibration of the subducting sediments could occur whilst leaving trace element ratios such a La/Ta unaffected. Kelemen et al. (1993) have argued that the depletion of HFSE such as Ta reflects melt – wall rock interaction during passage through the mantle wedge, however Elliott et al. (1997) have argued that this cannot be the case, at least in the Mariana arc, and in Kamchatka across-arc trends are the reverse of that predicted by such models (see later section).

In conclusion, it would appear that the development of the high La/Ta ratios in the Kamchatka lavas must, at least in part, reflect the melting process rather than source composition. This could be due to the presence of a residual HFSE-rich phase in the mantle wedge (e.g. Reagan and Gill 1989) or subducting slab, although experimental data (Ryerson and Watson 1987) suggest that at least rutile is unlikely to be stable in the mantle wedge. Similarly, the low Sr/Y ratios, absence of HREE depletion and the general contrast with the adakites from the northern segment suggest that the subducting slab is not undergoing partial melting beneath the EVF or CKD despite the MORB-like isotope ratios of the lavas and this is consistent with the age of the subducting crust and its implied cooler thermal structure. Thus, the negative Ta anomalies are unlikely to reflect the presence of a residual phase in the slab either. Thus, some other process must result in an increase of La/Ta from ~30 to 50–68 which would require that D_{La}/D_{Ta} = 0.06–0.11 for 10% partial melting. It should be noted that the present data do not allow us to rule out the possibility that no sediment is added in which case the observed La/Ta ratios reflect melting processes alone. Experimental partitioning data indicate that residual amphibole could fractionate La/Ta in the appropriate way with some recently published $D_{La}/D_{Ta \text{ or } Nb}$ values ranging from ~0.4 (La Tourrette et al. 1995; Klein et al. 1997) to < 0.04 (Ionov and Hofmann 1995). However, it remains to be shown independently that amphibole is a likely residual phase during mantle melting beneath island arcs.

The role and origin of slab-derived fluids

In most models, partial melting and magma genesis beneath island arcs is linked to the lowering of the peridotite solidus by the addition of aqueous fluids derived by dehydration of the subducting slab (e.g. Tatsumi et al. 1986; Davies and Stevenson 1992). Experimental mineral – aqueous fluid partitioning studies indicate that Ba, Pb, Sr, U and K are highly fluid mobile relative to the HFSE (e.g. Brenan et al. 1995; Keppler 1996). Thus, the high Ba/Th component in Fig. 9 is inferred to be aqueous fluid from the subducting slab (cf. Turner et al. 1996, 1997; Hawkesworth et al. 1997a, b). A significant observation from Fig. 9 is that this fluid component is characterised by $^{87}Sr/^{86}Sr$ ~0.7033 which is significantly less than that of the subducting sediments but greater than Pacific MORB, and variably low $^{206}Pb/^{204}Pb$ ~18.2–18.4 which overlaps the range for Pacific MORB. Analyses of altered MORB indicate that sea water interaction increases Rb, Ba, U, Sr and Pb concentrations as well as increasing $^{87}Sr/^{86}Sr$ ratios (range ~0.703–0.706) whereas Nd (and Pb) isotopes are unaffected (Staudigel et al. 1995). Thus, Fig. 9 suggests that the Sr and probably the majority of the Pb in the fluid component in the Kamchatka lavas was derived from the subducted altered oceanic crust (cf. Kersting and Arculus 1995) rather than the overlying sediments. This has also been observed in other arcs (Miller et al. 1994; Turner et al. 1996, 1997; Hawkesworth et al. 1997a,b) and, as indicated by the mixing curve in Fig. 9a, such diagrams have been used to argue for a three component model for island arc magma genesis since the fluid, mantle wedge and sediment components are effectively separated in Ba/Th-$^{87}Sr/^{86}Sr$ space.

As noted above, U is preferentially mobilised relative to Th in aqueous fluids (e.g. Bailey and Ragnarsdottir 1994; Brenan et al. 1995; Keppler 1996) and the ^{238}U-excesses observed in many young island arc rocks have accordingly been attributed to the addition of a slab-derived fluid (Gill and Williams 1990; McDermott and Hawkesworth 1991; Condomines and Sigmarsson 1993; Turner et al. 1996, 1997; Elliott et al. 1997; Hawkesworth et al. 1997a, b). Several lines of reasoning support this interpretation for the Kamchatka lavas. Firstly, the

Ba/Th arguments above strongly implicate the role of a fluid component. Secondly, a few of the Kamchatka lavas do have significant ^{238}U excesses (up to 23%). Thirdly, the Kamchatka data span a large range along the equiline in Fig. 5 with U/Th ratios consistently higher than those for either MORB or OIB but similar to the Lesser Antilles and Marianas arcs. In depleted island arcs like Tonga, departures from wedge – sediment mixing lines towards high U/Th and $^{208}Pb^*/^{206}Pb^*$ are interpreted to reflect addition of fluids derived from the altered oceanic crust in the down-going plate (Turner et al. 1997). Just such a trend is observed for Kamchatka in Fig. 9c suggesting that the high U/Th ratios similarly reflect fluid addition from altered oceanic crust. Given the evidence that the range to high U/Th reflects fluid addition, one of the unexpected results of this study is that the majority of the Kamchatka lavas lie on, or close to the equiline in Fig. 5, suggesting that the U-Th isotope disequilibria produced by this fluid addition was followed by return to the equiline by ^{230}Th-ingrowth as illustrated in the inset to Fig. 5. Note that in this model, the higher ($^{238}U/^{232}Th$) ratios of the CKD and northern EVF lavas relative to those of the southern EVF lavas therefore reflect a greater increase in U/Th ratio by fluid addition and this is consistent with the lack of any associated change in $^{143}Nd/^{144}Nd$. Finally, although there are fewer data, the Aleutian lavas form an array extending out to the right of the equiline on which those Kamchatka lavas that do preserve sizeable ^{238}U-excesses also lie (Fig. 5), consistent with fluid addition to the source of these lavas (see also Newman et al. 1984).

^{10}Be isotope systematics

Morris et al. (1990) have argued that the elevated $^{10}Be/^{9}Be$ ratios provide strong evidence for the incorporation of subducted oceanic sediment in the source of the Aleutian lavas. This is consistent with the low $^{143}Nd/^{144}Nd$ isotope ratios in these rocks (Fig. 4) and with the results of previous studies (e.g. Kay and Kay 1988). An important question arising from this study concerns the mechanism of transfer of the ^{10}Be signal. As discussed above, the ^{238}U-excesses reflect addition of a fluid component to the source of the Aleutian lavas. Therefore, although largely controlled by one point, the apparent positive correlation between ^{10}Be and ($^{238}U/^{230}Th$) in Fig. 6b suggests that although the ^{10}Be must originally derive from the upper parts of the subducted sediment pile, the majority observed in the arc lavas is picked up and transported into the mantle wedge by fluids derived from the altered oceanic crust. A similar conclusion was reached by Sigmarsson et al. (1990) when explaining a similar, positive correlation between ^{10}Be and ($^{238}U/^{230}Th$) in Andean lavas. Such a model is consistent with the high ^{10}Be being accompanied by elevated B/Be because B is highly fluid mobile (see discussion in Hawkesworth et al. 1997b), and is supported by studies of the Catalina schist which suggest that in subducted sediment packages Be and B are transported in aqueous fluids at depths of 20–50 km (Domanik et al. 1993). In this context, it is intriguing that the Kamchatka lavas do not have elevated $^{10}Be/^{9}Be$ ratios (Tera et al. 1990), since we have presented evidence that a fluid component was involved in their petrogenesis, and compared with the Aleutians, the rate of subduction is greater and the sediment thickness and composition similar. However, it is likely that the upper portions of the sediment, which would contain ^{10}Be, are being scraped off into the accretionary wedge instead of being subducted. In fact, the Nd and Pb isotope data may indicate that little or no sediment is being subducted beneath Kamchatka (Kersting and Arculus 1995). Alternatively, any ^{10}Be signal in the sediment component, but not the fluid component, has decayed since the time of subduction (see below).

Rates of element transfer

The U-series isotope data can be used to place constraints on the time elapsed since U/Th fractionation, caused by fluid addition to the mantle wedge, and partial melting and subsequent eruption. Recent studies of the Lesser Antilles, Tonga-Kermadec and Marianas arcs have suggested that this is of the order of 30 to 50 thousand years (Turner et al. 1996, 1997; Elliott et al. 1997). For example, Elliott et al. (1997) showed that lavas in the Marianas form a well defined U-Th pseudo-isochron with an age of 30 thousand years. A 30 thousand year reference line is illustrated in Fig. 5 passing through several of the Aleutian lavas suggesting similar time scales are involved there. Two Kamchatka lavas from the EVF volcanoes of Avachinsky and Vilyuchinsky also lie on the 30 thousand year reference line and such time scales probably require that fluid addition was the trigger for partial melting beneath these volcanoes (e.g. Elliott et al. 1997, but see also Dorendorf et al. 1997). However, as noted above, the striking observation is that the majority of the Kamchatka rocks lie close to the equiline, including the other sample from Avachinsky. If the earlier arguments that the range in ($^{238}U/^{232}Th$) reflects recent U addition by fluids are correct, it follows that the transfer time is much greater for the vast majority of the Kamchatka lavas and of the order of ≥150 thousand years (dashed reference line in Fig. 5). Nonetheless, the presence of small, but measurable ^{238}U-excesses in the greater majority of the Kamchatka lavas still indicates fluid addition occurred less than 350 thousand years ago thereby ruling out the possibility that these fluids contained a ^{10}Be signal which has since decayed. Conversely, if any sediment containing ^{10}Be was subducted and added to the source then this sediment component must have been transferred sufficiently slowly (i.e. several million years) that the ^{10}Be had decayed (see also Turner and Hawkesworth 1997; Hawkesworth et al. 1997b).

Across-arc variations

As noted in the introduction, Kamchatka provides a relatively rare opportunity to investigate across-arc variations. The distance from the trench for each volcano is estimated in Tables 1–3 (note that since the average angle of subduction is close to 45° beneath the peninsula or less nearer the trench, these distances approximate maximum distances above the Benioff zone) and these are plotted against several key trace element ratios in Fig. 10. Unfortunately, much of the trace element ratio variation in the data set presented here appears to be controlled by shallow level processes, allowing only broad generalisations to be made. Nonetheless, the lack of any systematic correlation between Sr, Nd or Pb isotopes and height above Benioff is symptomatic of the overall isotopic homogeneity of the Kamchatka arc.

As noted already, there is some evidence that the mantle wedge is slightly more depleted beneath the EVF due to melt extraction beneath the CKD. Consistent with this, there is some indication in Fig. 10a that Ce/Yb increases with distance from the trench, at least in the EVF volcanoes. However, increases in Ce/Yb across the arc might also reflect smaller degrees of melting occurring at increasing depths, possibly due to declining amounts of fluid addition (see below), as also inferred for the New Britain arc by Woodhead and Johnson (1993). Unfortunately, with the present data set we have found little evidence to distinguish between these two possibilities.

Previous studies have suggested that the fluid contribution decreases with depth in New Britain (Woodhead and Johnson 1993) and the Kuriles (Ryan et al. 1995; Ishikawa and Tera 1997). In Kamchatka, Ba/Th ratios, taken as a measure of the relative importance of the fluid contribution, remain consistently higher than MORB and there is little evidence that Ba/Th systematically decreases from the EVF to the CKD and Ichinsky volcano (Fig. 9b). However, the limited extent of active volcanicity on the Sredinny Ridge may indicate the cessation of fluid release from the slab occurs around 200–250 km depth about where white micas break down (e.g. Poli and Schmidt 1995). Alternatively, it may be that decreases in Ba/Th due to a declining fluid contribution are balanced by increases due to decreasing degrees of partial melting. Again, such alternatives are at present hard to distinguish. In some models the fluid traverses horizontally across the wedge from the slab (e.g. Davies and Stevenson 1992), although it is not yet clear how any hydrated peridotite can pass beyond the zone of partial melting beneath the volcanic front and yet remain hydrated subsequently to undergo partial melting beneath the CKD or Ichinsky. Although the dehydration of serpentinite in the altered oceanic crust is pressure dependant at around 2.3–2.5 Gpa, other hydrous minerals such as lawsonite and Mg-chloritoid may undergo semi-continuous breakdown and fluid release up to depths of 200 km (Poli and Schmidt 1995). Such protracted fluid release may provide an explanation for

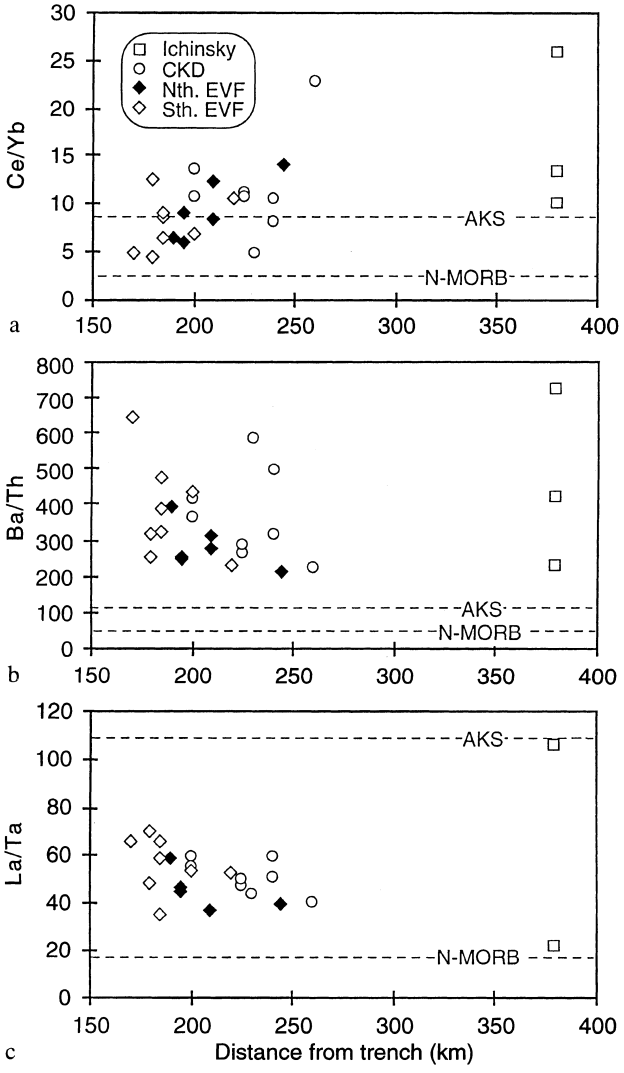

Fig. 10a-c Across-arc trends in Kamchatka: **a** Ce/Yb may show a broad increase suggesting either that the mantle wedge convecting beneath the arc front has been depleted by melt extraction beneath the CKD or else that the degrees of partial melting decrease towards the back arc. **b** Ba/Th shows little or no correlation with distance from the trench but is consistently higher than MORB or the average sediment (*AKS*) suggesting that the fluid contribution remains relatively constant. **c** La/Ta shows a possible decrease with distance from the trench but as Fig. 7a illustrates much of this is due to shallow level processes. Note that a positive correlation, which would be expected if melt – wall rock interaction controlled this ratio (Kelemen et al. 1993), is not observed. The *dashed lines* give the composition of MORB (Sun and McDonough 1989) and the average Kamchatka sediment (Plank and Langmuir 1998) for reference

back arc volcanism and if so this would suggest that partial melting occurs relatively close to the slab – mantle wedge interface.

Finally, it has been observed that the size of the negative HFSE anomaly, as measured by La/Ta, decreases with increasing depth to Benioff in both the New Britain arc (Woodhead and Johnson 1993) and in Japan (Ishikawa and Nakamura 1994). Clearly, this may be crucial to understanding the origin of HFSE anomalies in arc lavas. In Kamchatka, there is also a broad de-

crease in La/Ta with distance from the trench within each of the EVF and CKD groups towards MORB-like values (Fig. 10c). However as noted, much of the variation in La/Ta appears to be correlated with decreases in MgO and thus linked to shallow level crystal fractionation. If the high-MgO lavas alone are considered, then there is little or no evidence that La/Ta decreases across arc (see Fig. 7a). Although this may be an artefact of the limited number of high-MgO samples, there is a remarkable homogeneity in La/Ta (as well as radiogenic isotopes) in these high-MgO lavas. This would seem to suggest that the process responsible for the high La/Ta ratios causes similar La/Ta fractionation irrespective of distance from the trench or beneath the arc volcanoes. If residual amphibole is responsible for the high La/Ta ratios then the amount of amphibole (and by inference fluid addition) does not change significantly across the arc and, for reasons outlined above, this would appear to fit better with partial melting occurring close to the slab-wedge interface than with models in which fluids are translated horizontally across the wedge (Davies and Stevenson 1992). This, in turn, would seem to argue against models in which elevated La/Ta is produced by melt – wall rock interaction (Kelemen et al. 1993) since this model would predict that La/Ta would increase as the length of peridotite column traversed from slab to volcano increased; no such positive correlation is observed in Fig. 10c.

Concluding remarks

The lavas from the Kamchatka arc are striking in the homogeneity of their radiogenic isotopes. In contrast to data from the Aleutians, Nd and Pb isotope ratios overlap those for Pacific MORB and limit the amount of sediment that could be added to their mantle source region to $<1\%$ (cf. Kersting and Arculus 1995; Kepezhinskas et al. 1997). Given recent estimates of the composition of the average sediment being subducted beneath the arc, this is insufficient to account for the observed La/Ta ratios in the lavas. The lack of a positive correlation between La/Ta and depth to the slab suggests that melt – wall rock interaction was not important in controlling this ratio. Similarly, the low Sr/Y ratios, lack of HREE depletion, age of the descending plate and the contrast with lavas from the northern segment all argue against partial melting of the subducted oceanic crust. On the contrary, lavas from the northern segment, where the descending plate is young and hot and more likely to undergo melting, are characterised by a lack of a negative HFSE anomaly (Kepezhinskas et al. 1997). Thus, La/Ta ratios are inferred to have increased during partial melting requiring $D_{La}/D_{Ta} = 0.11$–0.06 which may reflect residual amphibole. The isotopic data would allow that no sediment is added to the source of the lavas (e.g. Kersting and Arculus 1995) in which case D_{La}/D_{Ta} would have to be lower still.

Ba, U, Sr and Pb were added to the source by an aqueous fluid from the subducting slab and the inferred Sr and Pb isotopic composition of this fluid indicates that it was derived from the altered oceanic crust (e.g. Miller et al. 1994; Turner et al. 1996, 1997). The addition of U resulted in U/Th isotope disequilibria however, the majority of samples now lie close to the equiline indicating that the time since U/Th fractionation is ≥150 thousand years. The present data reveal little or no systematic across-arc variation in radiogenic isotopes, La/Ta or Ba/Th. The large width of the volcanic zone is therefore assumed to represent protracted fluid release from the subducting slab over the depth interval 170–260 km. It may be that some minor fluid release still occurs at 380 km depth in order to explain the limited volcanism at Ichinsky.

The Aleutians data contrast strongly with those from Kamchatka. Radiogenic isotope data indicate that the Aleutian lavas contain a significant recycled sedimentary component, consistent with their elevated $^{10}Be/^{9}Be$ ratios (Morris et al. 1990). However, $^{10}Be/^{9}Be$ is positively correlated with ($^{238}U/^{230}Th$) suggesting that the ^{10}Be signal was carried by the aqueous fluid from the slab. The U/Th disequilibria for the Aleutian samples lie close to a 30 thousand year reference line suggesting that this fluid was released from the slab ~30 thousand years ago similar to estimates from the Lesser Antilles (Turner et al. 1996), Marianas (Elliott et al. 1997) and Tonga-Kermadec (Turner et al. 1997) island arcs. Given that the rate of convergence in Kamchatka is similar to that in the Marianas and Tonga-Kermadec the inferred greater time since fluid release is surprising and requires further investigation.

Acknowledgements We are particularly grateful to Jessica Bartlett, Mabs Gilmour, Rhiannon George, Nick Rogers and Peter van Calsteren for helping with the INAA and Sr, Nd and Pb isotope analyses. Julie Morris kindly provided the remnants of the Aleutian sample powders which had been analysed for Be and B. The manuscript was greatly improved by reviews from Kai Hoernle and Rob Ellam and by discussions with Gerhard Wörner. Research at the Open University is partly funded by the NERC and S.T. gratefully acknowledges the support of a Royal Society Research Fellowship.

References

Allègre CJ, Dupré B, Lewin E (1986) Thorium/uranium ratio of the Earth. Chem Geol 56: 219–227

Bailey EH, Ragnarsdottir KV (1994) Uranium and thorium solubilities in subduction zone fluids. Earth Planet Sci Lett: 124: 119–129

Bailey JC (1993) Geochemical history of sediments in the northwestern Pacific Ocean. Geochem J 27: 71–91

Baranov BV, Seliverstov NI, Murav'ev AV, Muzurov EL (1991) The Komondorsky Basin as a product of spreading behind a transform plate boundary. Tectonophysics 199: 237–269

Brenan JM, Shaw HF, Ryerson FJ, Phinney DL (1995) Mineral-aqueous fluid partitioning of trace elements at 900 °C and 2.0 Gpa: constraints on the trace element chemistry of mantle and deep crustal fluids. Geochim Cosmochim Acta 59: 3331–3350

Chabaux F, Allègre CL (1994) ^{238}U-^{230}Th-^{226}Ra disequilibria in volcanics: a new insight into melting conditions. Earth Planet Sci Lett 126: 61–74

Churikova T, Dorendorf F, Worner G, Eisenhauer A, Heuser A (1997) Across-arc variations in trace elements and U/Th isotopes in Kamchatka reveal intra-arc rifting and systematic geochemical zonation caused by fluids from the subducted oceanic crust. EOS Trans Am Geophys Union 78: 804

Condomines M, Sigmarsson O (1993) Why are so many arc magmas close to $^{238}U-^{230}Th$ radioactive equilibrium? Geochim Cosmochim Acta 57: 4491–4497

Davies JH, Stevenson DJ (1992) Physical model of source region of subduction zone volcanics. Geophys Res 97: 2037–2070

Domanik KJ, Hervig RL, Peacock SM (1993) Beryllium and boron in subduction zone minerals: an ion microprobe study. Geochim Cosmochim Acta 57: 4997–5010

Dorendorf F, Wiechert U, Wörner G, Puzankov M, Volynets O (1997) Strontium and oxygen isotope measurements on rocks from Kluchevskoy volcano (Kamchatka): evidence for melting a fluid-flushed mantle wedge. EOS Trans Am Geophys Union 78: 824.

Ellam RM, Hawkesworth CJ (1988) Elemental and isotopic variations in subduction related basalts: evidence for a three component model. Contrib Mineral Petrol 98: 72–80

Elliott T, Plank T, Zindler A, White W, Bourdon B (1997) Element transport from subducted slab to juvenile crust at the Mariana arc. J Geophys Res 102: 14991–15019

Ewart A, Hawkesworth CJ (1987) The Pleistocene–Recent Tonga–Kermadec arc lavas: interpretation of new isotopic and rare earth data in terms of a depleted mantle source model. J Petrol 28: 495–530

Geist EL, Scholl DW (1994) Large-scale deformation related to the collision of the Aleutian arc with Kamchatka. Tectonics 13: 538–560

Geist EL, Vallier TL, Scholl DW (1994) Origin, transport, and emplacement of an exotic island-arc terrane exposed in eastern Kamchatka, Russia. Geol Soc Am Bull 106: 1182–1194

Gill JB (1981) Orogenic andesites and plate tectonics. Springer-Verlag, Berlin Heidelberg New York Tokyo

Gill JB, Williams RW (1990) Th isotope and U-series studies of subduction-related volcanic rocks. Geochim Cosmochim Acta 54: 1427–1442

Gill JB, Morris JD, Johnson RW (1993) Timescale for producing the geochemical signature of island arc magmas: U-Th-Po and Be-B systematics in Recent Papua New Guinea lavas. Geochim Cosmochim Acta 57: 4269–4283

Goldstein SJ, Murrell MT, Janecky DR (1989) Th and U isotopic systematics of basalts from the Juan de Fuca and Gorda Ridges by mass spectrometry. Earth Planet Sci Lett 96: 134–146

Hawkesworth CJ, Hergt JM, McDermott F, Ellam RM (1991) Destructive margin magmatism and the contributions from the mantle wedge and subducted crust. Aust J Earth Sci 38: 577–594

Hawkesworth CJ, Gallagher K, Hergt JM, McDermott F (1993) Mantle and slab contributions in arc magmas. Annu Rev Earth Planet Sci 21: 175–204

Hawkesworth C, Turner S, Peate D, McDermott F, van Calsteren P (1997a) Elemental U and Th variations in island arc rocks: implications for U-series isotopes. Chem Geol 139: 207–222

Hawkesworth CJ, Turner SP, McDermott F, Peate DW, van Calsteren P (1997b) U-Th isotopes in arc magmas: implications for element transfer from the subducted crust. Science 276: 551–555

Hochstaedter AG, Kepezhinskas P, Defant M (1996) Insights into the volcanic arc mantle wedge from magnesian lavas from the Kamchatka arc. J Geophys Res 101: 697–712

Ionov DA, Hofmann AW (1995) Nb-Ta-rich mantle amphiboles and micas: implications for subduction-related metasomatic trace element fractionations. Earth Planet Sci Lett 131: 341–356

Ishikawa T, Nakamura E (1994) Origin of the slab component in arc lavas from across-arc variation of B and Pb isotopes. Nature 370: 205–208

Ishikawa T, Tera F (1997) Source, composition and distribution of the fluid in the Kurile mantle wedge: constraints from across-arc variations of B/Nb and B isotopes. Earth Planet Sci Lett 152: 123–138

Kay RW (1980) Volcanic arc magmas: implications of a melting-mixing model for element recycling in the crust-upper mantle system. J Geol 88: 497–522

Kay RW, Kay SM (1988) Crustal recycling and the Aleutian arc. Geochim Cosmochim Acta 52: 1351–1359

Kay RW, Sun SS, Lee-Hu CN (1978) Pb and Sr isotopes in volcanic rocks from the Aleutian Islands and Pribilof Islands, Alaska. Geochim Cosmochim Acta 42: 263–273

Kelemen PB, Shimizu N, Dunn T (1993) Relative depletion of niobium in some arc magmas and the continental crust: partitioning of K, Nb, La and Ce during melt/rock reaction in the upper mantle. Earth Planet Sci Lett 120: 111–134

Kepezhinskas P, Defant MJ, Drummond MS (1995) Na metasomatism in the island arc mantle by slab melt-peridotite interaction: evidence from mantle xenoliths in the north Kamchatka arc. J Petrol 36: 1505–1527

Kepezhinskas P, Defant MJ, Drummond MS (1996) Progressive enrichment of island arc mantle by melt-peridotite interaction inferred from Kamchatka xenoliths. Geochim Cosmochim Acta 60: 1217–1229

Kepezhinskas P, McDermott F, Defant MJ, Hochstaedter A, Drummond MS, Hawkesworth CJ, Koloskov A, Maury RC, Bellon H (1997) Trace element and Sr-Nd-Pb isotopic constraints on a three-component model of Kamchatka arc petrogenesis. Geochim Cosmochim Acta 61: 577–600

Keppler H (1996) Constraints from partitioning experiments on the composition of subduction-zone fluids. Nature 380: 237–240

Kersting AB (1995) Pb isotope ratios of North Pacific sediments, sites 881, 883 and 884: implications for sediment recycling in the Kamchatkan arc. In: Rea DK, Basov IA, Scholl DW, Allan JF (eds) Proc Ocean Drilling Program Sci Results 145, 383–389

Kersting AB, Arculus RJ (1994) Klyuchevskoy volcano, Kamchatka, Russia: the role of high-flux recharged, trapped, and fractionated magma chamber(s) in the genesis of high-Al_2O_3 from high-MgO basalt. J Petrol 35: 1–41

Kersting AB, Arculus RJ (1995) Pb isotope composition of Klyuchevskoy volcano, Kamchatka and North Pacific sediments: implications for magma genesis and crustal recycling in the Kamchatkan arc. Earth Planet Sci Lett 136: 133–148

Klein M, Stosch H-G, Seck HA (1997) Partitioning of high field-strength and rare-earth elements between amphibole and quartz-dioritic to tonalitic melts: as experimental study. Earth Planet Sci Lett 138: 257–271

LaTourrette T, Hervig RL, Holloway JR (1995) Trace element partitioning between amphibole, phlogopite, and basanite melt. Earth Planet Sci Lett 135: 13–30

McDermott F, Hawkesworth C (1991) Th, Pb, and Sr isotope variations in young island arc volcanics and oceanic sediments. Earth Planet Sci Lett 104: 1–15

McDermott F, Defant MJ, Hawkesworth CJ, Maury RC, Joron JL (1993) Isotope and trace element evidence for three component mixing in the genesis of the North Luzon arc lavas (Philippines). Contrib Mineral Petrol 113: 9–23

Miller DM, Goldstein SL, Langmuir CH (1994) Cerium/lead and lead isotope ratios in arc magmas and the enrichment of lead in the continents. Nature 368: 514–520

Morris JD, Leeman BW, Tera F (1990) The subducted component in island arc lavas: constraints from Be isotopes and B-Be systematics. Nature 344: 31–36

Newman S, Macdougall JD, Finkel RC (1984) ^{230}Th-^{238}U disequilibrium in island arcs: evidence from the Aleutians and the Marianas. Nature 308: 268–270

Pearce JA (1982) Trace element characteristics of lavas from destructive plate boundaries. In: Thorpe RS (ed) Orogenic andesites and related rocks. Wiley, New York, pp: 525–548

Pearce JA, Peate DW (1995) Tectonic implications of the composition of volcanic arc magmas. Annu Rev Earth Planet Sci 23: 251–285

Plank T, Johnson M (1997) Do subducted sediments melt beneath arc volcanoes? Some experimental answers (abstract). Geol Soc Aust Abstr 45: 76–78

Plank T, Langmuir CH (1998) The geochemical composition of subducting sediment and its consequences for the crust and mantle. Chem Geol 145: 325–394

Poli S, Schmidt WM (1995) H_2O transport and release in subduction zones: experimental constraints on basaltic and andesitic systems. J Geophys Res 100: 22299–22314

Rea DK (1993) Paleoceanographic record of North Pacific quantified. EOS Trans Am Geophys Union 74: 406–411

Reagan MK, Gill JB (1989) Coexisting calc-alkaline and high niobium basalts from Turialba volcano, Costa Rica: implications for residual titanites in arc magma sources. J Geophys Res 94: 4619–4663

Reagan MK, Morris JD, Herrstrom EA, Murrell MT (1994) Uranium series and beryllium isotope evidence for an extended history of subduction modification of the mantle below Nicaragua. Geochim Cosmochim Acta 58: 4199–4212

Ryan JG, Morris J, Tera F, Leeman WP, Tsvetkov A (1995) Cross-arc geochemical variations in the Kurile arc as a function of slab depth. Science 270: 625–627

Ryerson FJ, Watson EB (1987) Rutile saturation in magmas: implications for Ti-Nb-Ta depletion in island-arc basalts. Earth Planet Sci Lett 86: 225–239

Sigmarsson O, Condomines M, Morris JD, Harmon RS (1990) Uranium and ^{10}Be enrichments by fluids in Andean arc magmas. Nature 346: 163–165

Staudigel H, Davies GR, Hart SR, Marchant KM, Smith BM (1995) Large scale isotopic Sr, Nd and O isotopic anatomy of altered oceanic crust: DSDP Site 417/418. Earth Planet Sci Lett 130: 169–185

Stolper E, Newman S (1994) The role of water in the petrogenesis of Mariana trough magmas. Earth Planet Sci Lett 121: 293–325

Sun SS, McDonough WF (1989) Chemical and isotopic systematics of oceanic basalts: implications for mantle composition and processes. In: Saunders AD, Norry MJ (eds) Magmatism in ocean basins. Geol Soc Spec Publ 42: 313–345

Tatsumi Y, Hamilton DL, Nesbitt RW (1986) Chemical characteristics of fluid phase released from a subducted lithosphere and origin of arc magmas: evidence from high-pressure experiments and natural rocks. J Volcanol Geothermal Res 29: 293–309

Tera F, Morris JD, Leeman WP, Tsvetkov AA (1990) Further evidence from Be-B systematics for the homogeneity of the subducted component in arc magmatism: case of the Kurile-Kamchatka arc. Geochronol Isot Geol 27: 100

Todt W, Cliff RA, Hanser A, Hofmann AW (1993) Re-calibration of NBS lead standards using a $^{202}Pb + {}^{205}Pb$ double spike (abstract). Terra Abstr 5: 396

Turner S, Hawkesworth C (1997) Constraints on flux rates and mantle dynamics beneath island arcs from Tonga-Kermadec lava geochemistry. Nature 389: 568–573

Turner S, Hawkesworth C, van Calsteren P, Heath E, Macdonald R, Black S (1996) U-series isotopes and destructive plate margin magma genesis in the Lesser Antilles. Earth Planet Sci Lett 142: 191–207

Turner S, Hawkesworth C, Rogers N, Bartlett J, Worthington T, Hergt J, Pearce J, Smith I (1997) ^{238}U-^{230}Th disequilibria, magma petrogenesis and flux rates beneath the depleted Tonga-Kermadec island arc. Geochim Cosmochim Acta 61: 4855–4884

van Calsteren P, Schwieters JB (1995) Performance indications for TIMS with a deceleration lens system and post-deceleration detector selection. Int J Mass Spectrom Ion Proc 146/147: 119–129

Volynets O, Wörner G, Babansky A, Dorendorf F, Churikova T, Yogodzinsky G, Goltsman Y, Agapova A (1997) Variations in geochemistry and Sr-Nd isotopes in lavas from the northern volcanic group, Kamchatka: evidence for distinct sources at a subducting transform system. EOS Trans Am Geophys Union 78: 804

White WM, Hofmann AW, Puchelt H (1987) Isotope geochemistry of Pacific mid-ocean ridge basalt. J Geophys Res 92: 4881–4893

Woodhead JD, Johnson RW (1993) Isotopic and trace-element profiles across the New Britain island arc, Papua New Guinea. Contrib Mineral Petrol 113: 479–491